AGU PUBLICATIONS

Paleoceanography

RESEARCH ARTICLE
10.1002/2016PA003052

Key Points:
- Na/Ca of planktonic foraminifera collected alive from the Red Sea correlate positively with salinity
- The correlations of Na/Ca to salinity for G. ruber and G. sacculifer are similar (at least) up to S = 39.6

Supporting Information:
- Supporting Information S1

Correspondence to:
E. M. Mezger,
Eveline.Mezger@nioz.nl

Citation:
Mezger, E. M., L. J. de Nooijer, W. Boer, G. J. A. Brummer, and G. J. Reichart (2016), Salinity controls on Na incorporation in Red Sea planktonic foraminifera, *Paleoceanography*, *31*, 1562–1582, doi:10.1002/2016PA003052.

Received 8 NOV 2016
Accepted 19 NOV 2016
Accepted article online 24 NOV 2016
Published online 20 DEC 2016

The copyright line for this article was changed on 13 JAN 2017 after original online publication.

Salinity controls on Na incorporation in Red Sea planktonic foraminifera

E. M. Mezger[1], L. J. de Nooijer[1], W. Boer[1], G. J. A. Brummer[1,2], and G. J. Reichart[1,3]

[1]Department of Ocean System Sciences, Royal Netherlands Institute for Sea Research, and Utrecht University, Texel, Netherlands, [2]Faculty of Earth and Life Sciences, Department of Earth Sciences, Cluster Earth and Climate, VU University Amsterdam, Amsterdam, Netherlands, [3]Faculty of Geosciences, Department of Earth Sciences, Utrecht University, Utrecht, Netherlands

Abstract Whereas several well-established proxies are available for reconstructing past temperatures, salinity remains challenging to assess. Reconstructions based on the combination of (in)organic temperature proxies and foraminiferal stable oxygen isotopes result in relatively large uncertainties, which may be reduced by application of a direct salinity proxy. Cultured benthic and planktonic foraminifera showed that Na incorporation in foraminiferal shell calcite provides a potential independent proxy for salinity. Here we present the first field calibration of such a potential proxy. Living planktonic foraminiferal specimens from the Red Sea surface waters were collected and analyzed for their Na/Ca content using laser ablation quadrupole inductively coupled plasma mass spectrometry. Using the Red Sea as a natural laboratory, the calibration covers a broad range of salinities over a steep gradient within the same water mass. For both *Globigerinoides ruber* and *Globigerinoides sacculifer* calcite Na/Ca increases with salinity, albeit with a relatively large intraspecimen and interspecimen variability. The field-based calibration is similar for both species from a salinity of ~36.8 up to ~39.6, while values for *G. sacculifer* deviate from this trend in the northernmost transect. It is hypothesized that the foraminifera in the northernmost part of the Red Sea are (partly) expatriated and hence should be excluded from the Na/Ca-salinity calibration. Incorporation of Na in foraminiferal calcite therefore provides a potential proxy for salinity, although species-specific calibrations are still required and more research on the effect of temperature is needed.

1. Introduction

Seawater salinity is set by several processes, including river discharge, waxing and waning of continental ice sheets, sea ice formation, and the balance between evaporation and precipitation. Salinity, together with temperature, plays a major role in setting sea water density, determining seawater circulation patterns both on a global and regional scale. This makes salinity one of the key parameters for reconstructing past ocean functioning and its relation to past climate. At the same time, a proxy for salinity is necessary to correct for the impact of salinity on other proxies, for example, temperature reconstructions based on foraminiferal shell $\delta^{18}O$ [*Rohling*, 2007] and Mg/Ca [e.g., *Dissard et al.*, 2010]. Current reconstructions of past salinity are mostly based on combining stable isotopes (e.g., δD of long chained ketones or foraminiferal $\delta^{18}O$) with independent reconstructions for seawater temperature (e.g., foraminiferal Mg/Ca or $U^{k'}_{37}$) [*Elderfield and Ganssen*, 2000; *Schouten et al.*, 2006]. The uncertainty in these calibrations and the independent controls on these proxy signals leads to error propagation which effectively makes most of these approaches hard to apply [*Rohling*, 2007]. One of the uncertainties is based on the assumption that the relation between seawater stable isotopes and salinity remained constant over the time interval studied. On geological timescales, however, this relation likely varied, as it does spatially [e.g., *Gat*, 1996; *Zahn and Mix*, 1991]. To circumvent this problem, the relation between salinity and stable isotopes is often modeled [e.g., *Rohling and Bigg*, 1998], using assumptions on several hydrological factors and thereby increasing the uncertainty in reconstructed salinity.

Ideally, a proxy for salinity directly depends on the elements that determine ocean salinity, e.g., Na, Cl, and K, or is covarying strongly with salinity. For several elements, a direct relation was found between the element/Ca ratio in foraminiferal calcite and that in the ambient seawater (e.g., Mg/Ca [*Segev and Erez*, 2006; *Evans et al.*, 2015], Ba/Ca [*Hönisch et al.*, 2011], Cu/Ca [*De Nooijer et al.*, 2007], and Ba/Ca [*Lea and Boyle*, 1991]). For some (e.g., conservative) elements, their incorporation is generally dependent not (only) on the concentration of these elements in seawater but (also) on other environmental factors, such as

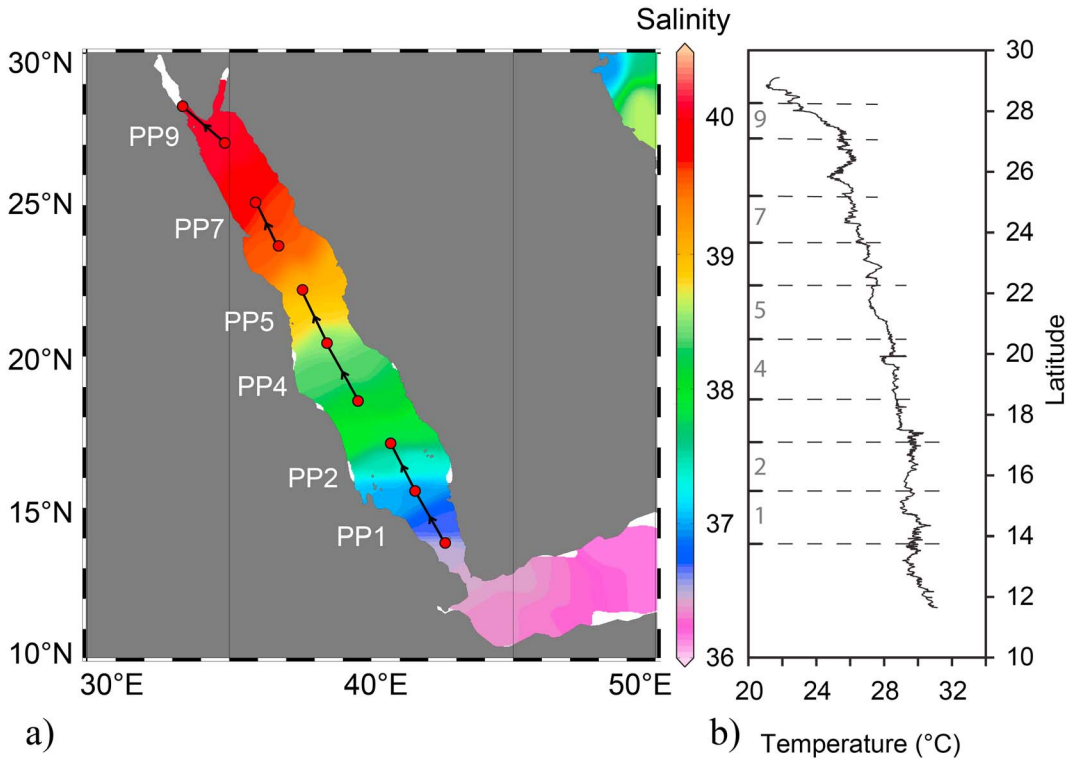

Figure 1. Salinity map (WOA 2001, average April–June) with (a) annual average salinities of the Red Sea and (b) aquaflow temperatures for the used plankton pump (PP) transects of R/V *Pelagia* cruise 64PE158. To the left of the temperature graph, the PP samples are also indicated.

temperature (Mg/Ca [e.g., *Anand et al.*, 2003; *Nürnberg et al.*, 1996]) or pH (B/Ca [*Yu et al.*, 2007, and references therein]). Na incorporation was found to be correlated to salinity in the carbonate of Atlantic oysters [*Rucker and Valentine*, 1961] and barnacle shells [*Gordon et al.*, 1970]. For inorganically precipitated calcite and aragonite this relation was shown to be dependent on Na concentration rather than the medium's Na/Ca ratio [*Kitano et al.*, 1975; *Ishikawa and Ichikuni*, 1984]. Recently, it was found that the [Na+] composition of calcite of cultured benthic and planktonic species of foraminifera also positively correlates with salinity (*Wit et al.* [2013] and *Allen et al.* [2016], respectively), which was explained by a relative increase in activity of free [Na^{+}] compared to [Ca^{2+}] activity with increasing salinity [*Wit et al.*, 2013]. Robust application of this proxy would, however, require finding this relationship in other cultured species (planktonic and benthic) and in the natural environment. For this purpose, we investigate Na/Ca of living planktonic foraminifera collected across a steep salinity gradient in the Red Sea. The Red Sea provides a natural laboratory with a broad salinity range (36 to 40), from which living specimens of the planktonic foraminifera *Globigerinoides ruber* (white) and *Globigerinoides sacculifer* were analyzed for their Na/Ca composition.

2. Materials and Methods

2.1. Study Area and Sample Collection

The Red Sea, with a total length of approximately 2100 km, is enclosed by deserts (Figure 1). The only connection to the open ocean is through the shallow and narrow straits of Bab el Mandeb, connecting the Red Sea with the Gulf of Aden and ultimately the Indian Ocean. Due to the very high evaporation rates in this basin (up to ~2 m/yr) [*Sofianos et al.*, 2002, *Morcos*, 1970], low mean annual rainfall from 3 mm/yr (N) to 150 mm/yr (S) [*Zahran*, 2010] and no significant rivers flowing into the basin, the basin is characterized by a pronounced antiestuarine circulation [*Rohling*, 1994, and references therein]. Surface waters flow northward while evaporating, resulting in a strong south-north gradient in salinity. Monsoonal winds cause seasonal contrasts, also influencing exchange through Bab el Mandeb. During the summer monsoon, circulation becomes three layered due to a wind-driven upper surface layer flowing into the Gulf of Aden [*Siccha et al.*, 2009, and

Table 1. Details per Transect[a]

Transect	Latitude Begin–End (°N)	Longitude Begin–End (°E)	Average SSS	Average SST	TA	DIC	CO_3^{2-}	pH
PP1	14.16–15.66	42.36–41.46	36.8	29.5	2333.6	2043.3	208.0	7.93
PP2	15.66–17.12	41.46–40.47	37.3	29.4	2354.6	2051.6	216.3	7.94
PP4	19.06–20.57	39.10–38.21	38.4	28.5	2370.6	2061.9	219.3	7.95
PP5	20.57–22.29	38.21–37.46	38.8	28.0	2376.5	2065.4	220.4	7.95
PP7	23.70–25.40	37.78–35.68	39.6	26.3	2409.2	2084.1	229.1	7.99
PP9	27.03–28.49	34.67–33.14	40.1	24.2	2425.7	2107.6	224.1	8.00

[a]Temperatures (sea surface temperature), alkalinities (TA), and dissolved inorganic carbon (DIC) were measured during RV *Pelagia* cruise 64PE158. Sea surface salinities (SSS) were obtained from the world ocean atlas (WOA_2001_average April–June *Boyer et al.* [2005]). Carbonate ion content (CO_3^{2-}) and pH values were calculated from the measured DIC and TA values using CO2SYS [*Lewis and Wallace*, 1998].

references therein]. This change in monsoonal strength between summer and winter does not affect salinities noticeably (World Ocean Atlas (WOA) 2001) [*Boyer et al.*, 2005]. However, maximum temperatures become ~2°C lower at the southernmost position [*Boyer et al.*, 2005]. The temperature gradient opposes the salinity gradient, with temperatures increasing from north to south. Still, to avoid as much as possible offsets in calibration due to such minor variations in salinity, we here calibrate to seasonal salinity data (April–June 2001). The carbonate ion content (CO_3^{2-}) and pH were calculated from measured dissolved inorganic carbon (DIC) and alkalinity (TA) values recorded during the cruise, using CO2SYS software [*Lewis and Wallace,* 1998].

Nine plankton pump (PP) samples were collected in May 2000 (RV *Pelagia* cruise 64PE158), with each sampling interval covering ~225 km on the S to N transect (Figure 1). Aquaflow sea surface temperatures were continuously recorded during the cruise, whereas salinity data were retrieved from average values from April to June from the World Ocean Atlas 2001 (WOA01; Table 1) [*Boyer et al.*, 2005]. Salinity measurements from CTD casts at five stations were available, with salinity values in close agreement with those obtained from the WOA01 database. Upon collection samples were sieved over a 75 μm mesh, shortly rinsed with ultrapure water to remove the salts and stored at −40°C. Subsequently, samples were freeze dried and a low-temperature asher was used to concentrate the foraminiferal specimens and remove organic matter (for samples PP2, PP4, and PP7) [*Fallet et al.*, 2009]. After ashing, samples were treated with a few drops of ethanol and ultrapure water to disaggregate the residue, wet sieved over a 63 μm mesh, and dried. Samples PP1, PP5, and PP9 were processed earlier and treated differently: after defrosting the samples, organic matter was removed using hot alkaline H_2O_2 for several hours based on the protocol of *Fallet et al.* [2009], after which they were rinsed three times with ultrapure water, ultrasonicated with each rinse and dried. *Fallet et al.* [2009] showed that both methods successfully remove all organic material from foraminiferal shells and yield equal isotope and Mg/Ca values. No offsets in averages for the measured elements were observed between the different methods and scanning electron microscopy (Hitachi, SEM3000) pictures showed a clean foraminiferal surface with no organic films remaining (Figure 2). Foraminifera were handpicked and species identified using the species concept of *Brummer et al.* [1987] for *G. sacculifer* (Brady) and *G. ruber* (d'Orbigny). Foraminiferal sizes were determined by measuring the diameter, from the top of the final chamber (F) to the bottom. Calculating chamber number in the size fraction employed here (100–460 μm) is very challenging: only a small change in diameter may offset the chamber number appreciably [*Brummer et al.*, 1987]. This is due to the exponential increase in size with chamber number [e.g., *Hemleben and Bijma*, 1994; *Brummer et al.*, 1987]. Based on measured sizes, the chamber number was determined for *G. sacculifer* using the study of *Hemleben and Bijma* [1994]. For *G. ruber*, there is unfortunately no such study to base the chamber number over the measured size range. Therefore, we used an extrapolation of the ontogenetic measurements given by *Brummer et al.* [1987] to estimate the chamber number.

2.2. LA-Q-ICP-MS Analyses

Prior to analysis, the foraminifera isolated from the plankton pump samples were cleaned with ultrapure water (>18.2 MΩ) and mounted on a stub with double-sided tape. Elemental composition of their calcite was measured by laser ablation quadrupole inductively coupled plasma mass spectrometry (LA-Q-ICP-MS) at the Royal NIOZ (Figure 2). This setup consists of a NWR193UC (New Wave Research) laser, containing an

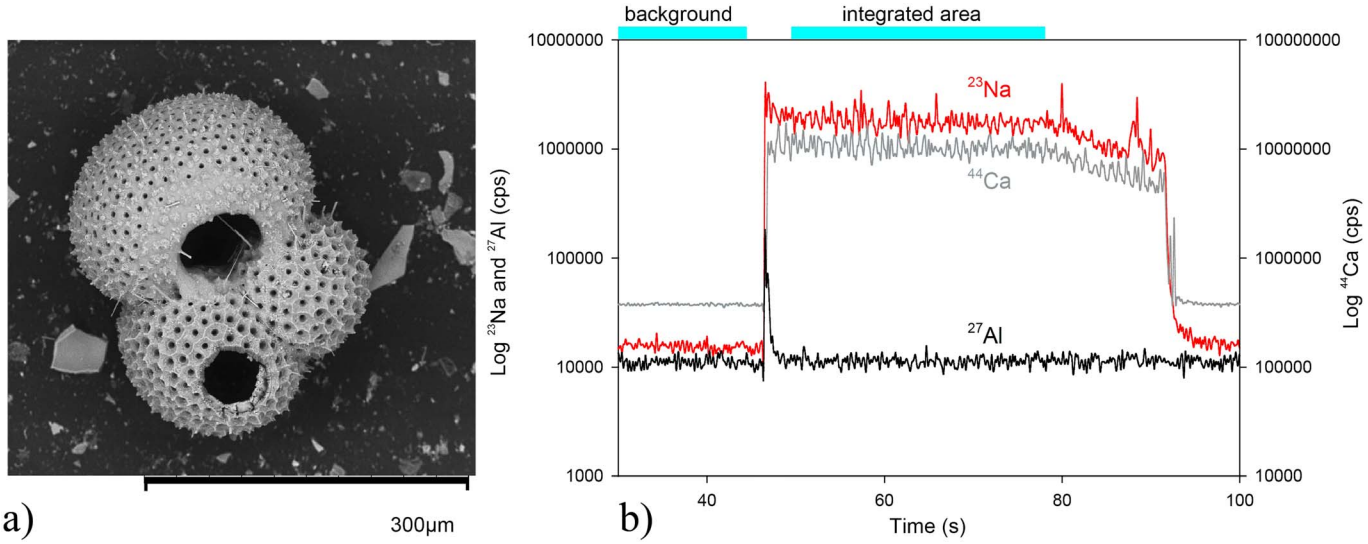

Figure 2. Example of (a) a laser ablated specimen of *G. ruber* and (b) the corresponding laser ablation profile with values for Na, Al, and Ca in counts per second.

ArF Excimer laser (Existar) with deep UV 193 nm wavelength and <4 ns pulse duration, coupled to a quadrupole ICP-MS (iCAP-Q, Thermo Scientific). Laser ablation of calcite was performed with a circular spot size of 60 µm and a fluence of 1 J/cm^2 at a repetition rate of 6 Hz. A fluence higher than 1 J/cm^2 increases the ablation rate and hence limits the run time length. For the glass NIST-610 and NIST-612 standards, the ablation threshold is at a fluence of 1 J/cm^2 [*Brokmann et al.*, 2002; *Hülsenberg et al.*, 2008]. However, since ablation just above this threshold potentially causes fractionation and the fractionation index of Na and Ca remains constant over the range 5–19 J/m^2 [*Li et al.*, 2015], a fluence of 5 J/cm^2 is used. This difference in fluence is shown not to influence the results [*Dueñas-Bohórquez et al.*, 2011; *Hathorne et al.*, 2008]. All samples were ablated for between 40 to 60 s, depending on the chamber thickness and size of the shell. The laser ablation system was equipped with a dual-volume cell, using helium as a carrier gas with a flow rate of 0.7 L/min. The optimum He flow was determined by several tests, focusing on stability of the signal, intensity, peak shape, and washout time. Between the ablation cell and mass spectrometer, a smoother was placed to avoid interferences between ablation pulses and cycle time of the MS [*Fehrenbacher et al.*, 2015]. From the laser chamber to the ICP-MS, the He flow was mixed with ~0.4 L/min Ar makeup gas and 0.003 mL/min N_2. Before measuring the samples, the makeup gas, extraction lens, focus lens, and torch position were automatically tuned for the highest sensitivity of ^{238}U, ^{139}La, ^{59}Co, and low ThO/Th ratios (<0.5%) by laser-ablating NIST-610 glass. The masses measured by the ICP-MS were ^{11}B, ^{23}Na, ^{24}Mg, ^{25}Mg, ^{27}Al, ^{39}K, ^{43}Ca, ^{44}Ca, ^{55}Mn, ^{57}Fe, ^{88}Sr, ^{138}Ba, and ^{238}U. The duration of one cycle of these 13 isotopes was 0.13 s. Every sample run lasted approximately 100 s, of which the first 20 s consisted of a gas blank. Intensity data were integrated, background subtracted, standardized internally to ^{43}Ca and calibrated against the NIST-610 signal using Thermo Qtegra software version 2.2.1465.44 and reference values from *Jochum et al.* [2011]. Since ablation of the NIST-610 and NIST-612 standards could increase the sodium background, they were only ablated and analyzed at the end of every sequence and cones were cleaned before the next sequence. The powders JCp-1, the synthetic $CaCO_3$ MACS-3, and an in-house (foraminiferal) calcite standard (NFHS-1, supporting information Text S1) were pressed to a tablet and used for monitoring drift and quality control and measured every 10 foraminiferal samples [*Okai et al.*, 2002; *Wilson et al.*, 2008]. The NFHS-1 standard was made primarily to create a powdered standard as close as possible in composition to foraminiferal calcium carbonate (Na/Ca: ~3–12 mmol/mol).

Relative precision of the Na/Ca analyses was better than 9%, based on the three different calcium carbonate standards (two international, one in-house) used (MACS-3: 27.5 ± 0.8 mmol/mol Na/Ca; JCp-1: 19.5 ± 1.4 mmol/mol Na/Ca; NFHS-1: 5.8 ± 0.5 mmol/mol Na/Ca). Accuracy of the analyses, based on comparing the carbonate standards with internationally reported values [*Okai et al.*, 2002; *Wilson et al.*, 2008], was 101 ± 3% and 97 ± 7% for MACS-3 and JCp-1, respectively. The measurements of Mg and Na per

standard were also normally distributed, except for Mg for the NFHS-1 (supporting information Figure S1 and Table S1). The fact that the NFHS-1 is not normally distributed is somewhat puzzling. It does suggest multiple phases of carbonate present (i.e., low and high Mg carbonates) but is here irrelevant due to the very small grain size (<1 μm) the standard was ground to (supporting information Text S1).

A comparison of our data with solution sector field inductively coupled plasma mass spectrometry (SF-ICP-MS, Thermo Scientific, Element-2) shows no offsets caused by laser ablation (supporting information Text S2, Figure S2, and Tables S2 and S3). We compared these two methods on standard material and artificial pressed pellets with a Na addition series. The linearity ($r^2 = 0.99$) of the plot and the slope of 0.98 indicate that LA-Q-ICP-MS delivers accurate Na/Ca data. Although the very low Na/Ca values for the lower part of the intercomparison are somewhat off, these values are much lower than the range found for foraminifera (3–12 mmol/mol). With concentrations similar to those found for foraminiferal carbonate, Na/Ca values are very close to the reference and solution analyses based values.

2.3. Data Processing

Foraminiferal signals were screened for surface contamination, and parts of the outside or inside of the shell with elevated Mg, often accompanied by a small peak in Na and Al, were eliminated from the area selected for integration. Since shells were collected from living specimens and have never been in contact with the sediment, surface contaminations must be caused during the sample processing. Measurements were discarded in cases when the shell (test) wall was very thin and the analytical sequence was too short (<5 s). Only the last three shell chambers were analyzed to minimize potential impacts of migration of the collected specimens. Outliers are identified routinely by the average −2SD and average +2SD per transect. In total 153 specimens of *G. ruber* (white) were analyzed, varying between 5 and 50 per transect. For *G. ruber* a total of 171 analyses, including duplicates and outliers, provided the data for calculating the average foraminiferal shell chemical composition per transect (Figures 3–5, and S3–S8). For *G. sacculifer*, in total 46 specimens were analyzed, varying between 2 and 19 specimens per transect, to a total of 70 single-spot analyses including outliers and duplicates. No significant differences were found between the analyzed chambers' position (respectively F and F-1). Values deviating from the average by more than twice the standard deviation of the whole population of a species per transect were considered outliers and excluded from further calculations. Even though the internal variability expressed as relative standard deviation (RSD(%) = average/SD × 100) per single-spot analysis for Mg/Ca was relatively high with an average below 40% for both species, the standard error of the mean (= RSD/$\sqrt{n}$) per single-spot measurement was ~2.5%. For Sr/Ca, the variability per measurement was below 30% on average for both species with a standard error of ~1.8%. The variability per single-spot measurement for Na/Ca was always less than 35% for both species with a standard error of ~2.1%.

Ratios for Mg/Ca, Sr/Ca, and Na/Ca per sampled transect are either normally or randomly distributed for both *G. sacculifer* and *G. ruber* (supporting information Figures S3–S8 and Table S4 and S5). Relative standard deviations for these elements per group of single-spot analyses per transect vary around 10%, which is close to the analytical error. Due to the large number of replicates, standard errors are considerably lower (Table 2). Before calculating correlations or applying statistics, elemental ratios for both species per transect were first tested for normality with the Shapiro-Wilk test.

3. Results

3.1. Na/Ca

Values for single-chamber Na/Ca for *G. ruber* are either normally distributed within transects (PP1, PP2, PP5, and PP9), slightly skewed (PP7), or randomly (PP4) distributed (supporting information Figure S3 and Table S4). However, despite the positive results for PP9 Na/Ca values in the Shapiro-Wilk test, the distribution appears randomly instead of normally distributed. Standard deviations within transects vary from 8 to 17% (Table 2). For *G. sacculifer*, Na/Ca values are normally distributed for all transects except for PP7, with standard deviations varying between 4 to 14% (supporting information Figure S6 and Table 2 and supporting information Table S5).

A significant positive correlation is found between salinity and average Na/Ca values for *G. ruber*, while for *G. sacculifer* only a positive trend is observed (Figure 3). Linear regressions equal: Na/Ca = 0.66 × S–15.75

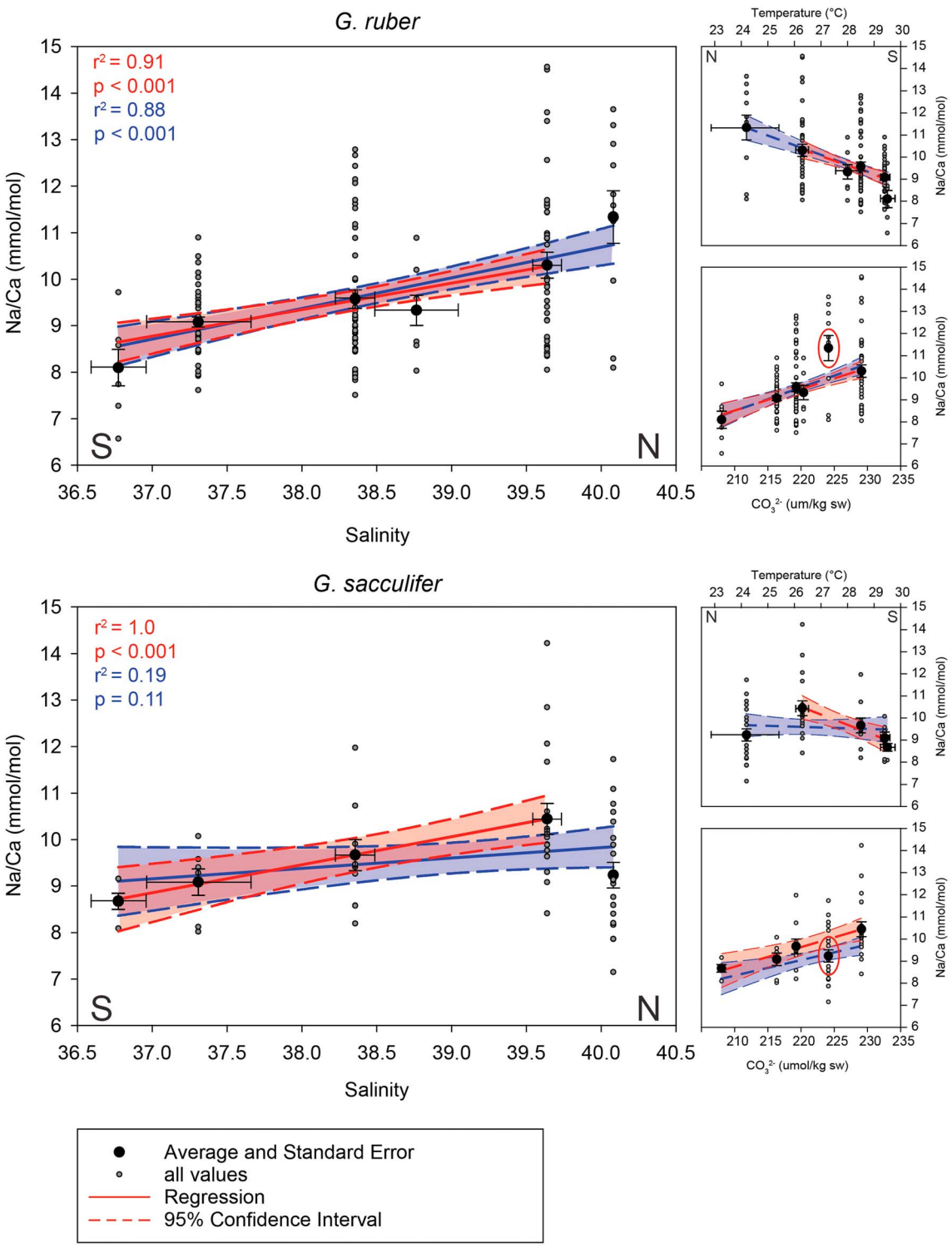

Figure 3. *G. ruber* and *G. sacculifer* Na/Ca values, plotted against salinity (WOA01, average April–June), measured temperatures, and calculated CO_3^{2-}. For reasons further explained in the discussion (section 4.1.2), all calibrations are given with (blue) and without (red) the northernmost transect. The r^2 value was calculated using weighted averages and shaded areas around the calibrations indicate the 95% confidence interval of the regressions. Horizontal error bars for salinity and temperature indicate values recorded at the start and end of each transect. Vertical error bars are the standard errors of the mean. (right column) Note that the south (S) to north (N) scales are reversed for the two temperature plots. For the Na/Ca-temperature relationship, excluding the northernmost transect results in r^2 values of 0.84 and $p < 0.001$ for *G. ruber* and $r^2 = 0.95$ and $p < 0.001$ for *G. sacculifer*. When including the northernmost transect, the Na/Ca-temperature relationship has an r^2 of 0.90 and $p < 0.001$ for *G. ruber* and $r^2 = 0.02$ and $p = 0.56$ for *G. sacculifer*. For the Na/Ca-CO_3^{2-} correlation, $r^2 = 0.92$ and $p < 0.001$ for *G. ruber* and $r^2 = 0.97$ with $p < 0.001$ for *G. sacculifer*. When including the northernmost transect, the Na/Ca-CO_3^{2-} relationship has an r^2 of 0.71 and $p < 0.001$ for *G. ruber* and $r^2 = 0.64$ and $p = 0.003$ for *G. sacculifer*.

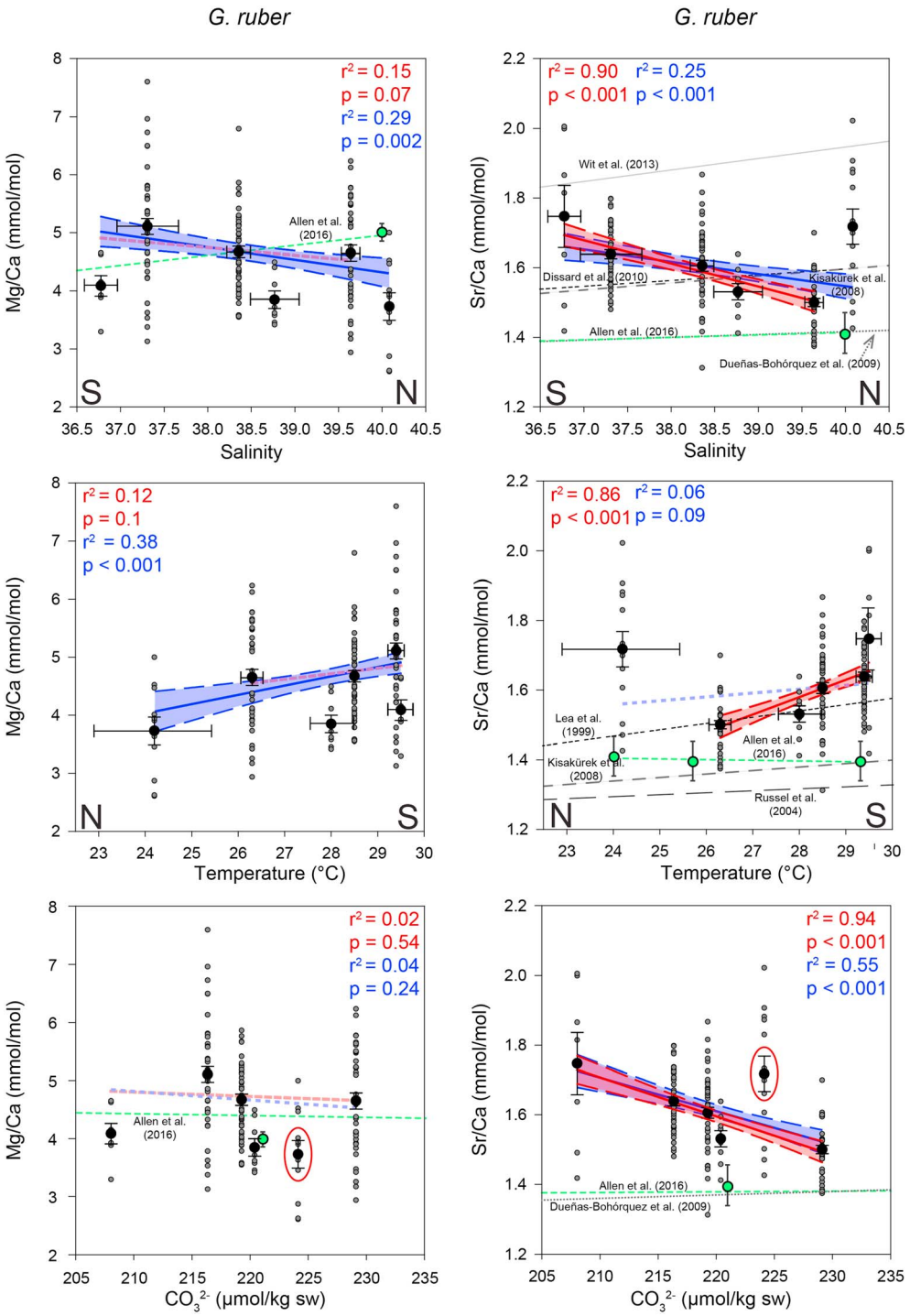

Figure 4. Sr/Ca and Mg/Ca values for *G. ruber*, plotted against salinity (WOA01, average April–June), measured temperatures and calculated CO_3^{2-}. Nonsignificant calibrations from this study are indicated in light blue (including northernmost transect) and light pink (excluding the northernmost transect) dotted trend lines. Other Sr/Ca-temperature and salinity correlations are from *Wit et al.* [2013] and *Dissard et al.* [2010] for *A. tepida*, *Kısakürek et al.* [2008] for *G. ruber*, *Dueñas-Bohórquez et al.* [2009] for *G. sacculifer*, and *G. ruber* and *O. universa* combined and *Russel* et al. [2004] for *O. universa*. The red ovals indicate the northernmost transect in the CO_3^{2-} plots. The green dots with analytical errors and green dotted lines give the data of *Allen et al.* [2016] for *G. sacculifer* and *G. ruber*. For further explanations, see caption of Figure 3.

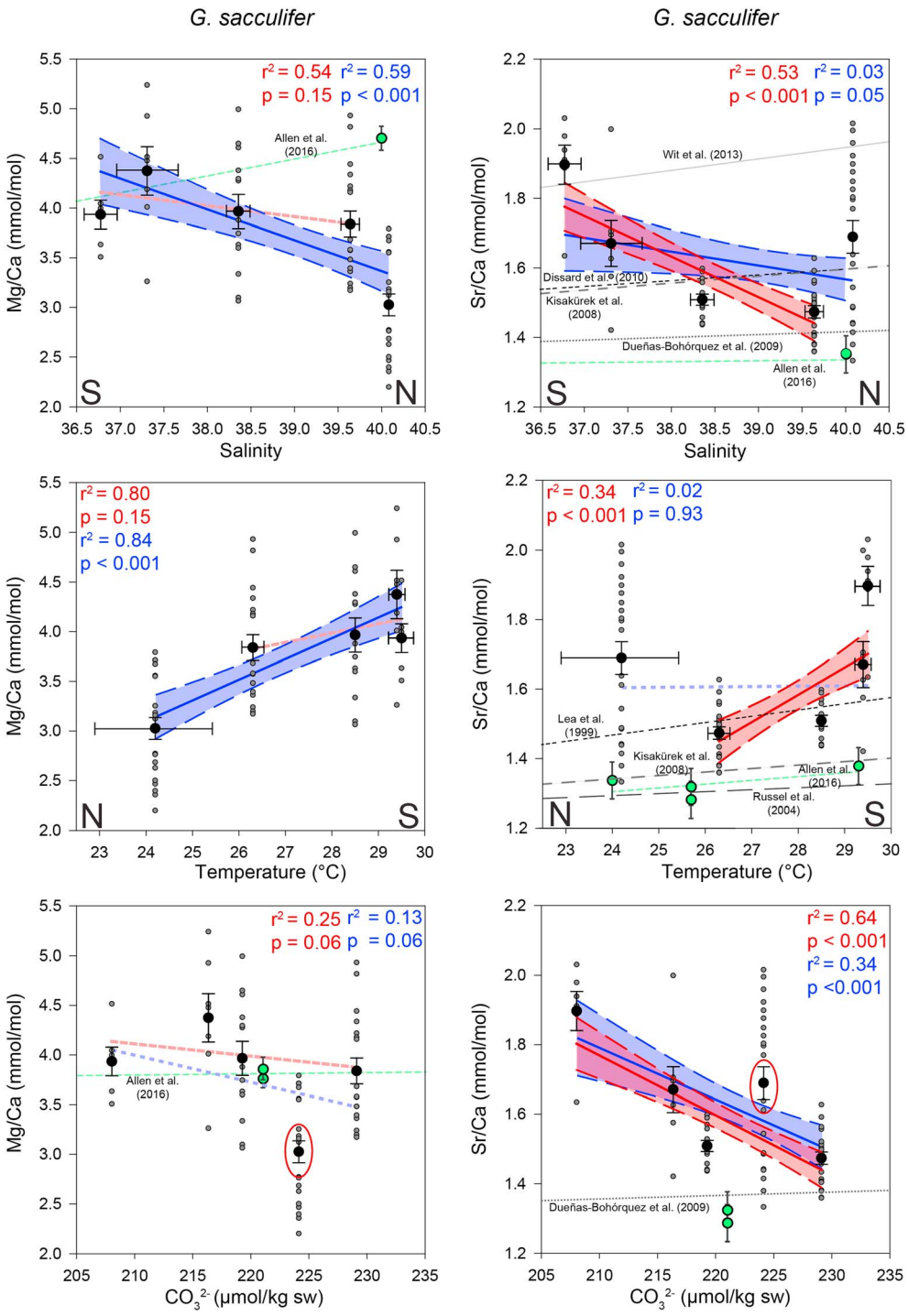

Figure 5. Sr/Ca and Mg/Ca values for *G. sacculifer*, plotted against salinity (WOA01, average April–June), measured temperatures and calculated CO_3^{2-}. For further explanations, see captions of Figures 3 and 4.

($r^2 = 0.88$, $p < 0.001$) for *G. ruber* and the nonsignificant Na/Ca = 0.229 × S + 0.67 ($r^2 = 0.19$, $p = 0.11$) for *G. sacculifer*. Na/Ca of both species follows the same positive trend up to a salinity of 39.6, while values for the northernmost transect PP9 for *G. sacculifer* deviate strongly from this trend. When excluding the northernmost transect (section 4.1.2), linear regressions equal Na/Ca = 0.57 × S–12.38 ($r^2 = 0.91$, $p < 0.001$) for *G. ruber* and Na/Ca = 0.60 × S–13.49 ($r^2 = 0.999$, $p < 0.001$) for *G. sacculifer*.

Table 2. Mg/Ca, Sr/Ca, and Na/Ca Values for *G. ruber* and *G. sacculifer*[a]

		Mg/Ca				Sr/Ca				Na/Ca			
Species	Salinity	mmol/mol	*n*	2 × SD	SE	mmol/mol	*n*	2 × SD	SE	mmol/mol	*n*	2 × SD	SE
G. ruber	36.8	4.09	7	0.93	0.35	1.75	7	0.47	0.18	8.10	7	2.06	0.39
G. sacculifer		3.93	6	0.71	0.27	1.90	6	0.28	0.11	8.67	5	0.76	0.17
G. ruber	37.3	5.11	45	1.84	0.69	1.64	43	0.17	0.03	9.07	43	1.42	0.11
G. sacculifer		4.37	7	1.21	0.46	1.67	7	0.35	0.13	9.08	7	1.51	0.29
G. ruber	38.4	4.67	49	1.38	0.52	1.61	50	0.22	0.03	9.57	51	2.87	0.20
G. sacculifer		3.97	13	1.24	0.47	1.51	13	0.12	0.03	9.66	10	2.13	0.34
G. ruber	38.8	3.85	8	0.85	0.32	1.53	9	0.14	0.05	9.33	8	1.85	0.33
G. ruber	39.6	4.65	39	1.74	0.66	1.50	37	0.15	0.02	10.30	39	3.49	0.28
G. sacculifer		3.84	18	1.10	0.42	1.47	20	0.16	0.04	10.45	18	2.84	0.33
G. ruber	40.1	3.73	11	1.58	0.60	1.72	13	0.37	0.10	11.34	11	3.74	0.56
G. sacculifer		3.03	21	1.01	0.38	1.69	22	0.44	0.09	9.23	20	2.48	0.28

[a]Standard deviations (SD), standard errors (SE = $\sigma/\sqrt{n}$), and number of specimens per transect (*n*).

Since salinity and temperature are anticorrelated in our data set, increasing Na/Ca toward the North of the Red Sea may also be interpreted as a negative correlation between Na/Ca and temperature. When including the northernmost transect, the correlation between Na/Ca and temperature has an r^2 of 0.90 for *G. ruber*, $p < 0.001$, and $r^2 = 0.02$, and $p = 0.56$ for *G. sacculifer*. The relationship between Na/Ca and temperature, when excluding the northernmost transect (Figure 3), has r^2 values of 0.84 and $p < 0.001$ for *G. ruber* and $r^2 = 0.95$ and $p < 0.001$ for *G. sacculifer*. For the correlation between Na/Ca and CO_3^{2-}, $r^2 = 0.71$ and $p < 0.001$ for *G. ruber*, and $r^2 = 0.64$ and $p = 0.003$ for *G. sacculifer*. When excluding PP9, $r^2 = 0.92$ and $p < 0.001$ for *G. ruber* and $r^2 = 0.97$ with a $p < 0.001$ for *G. sacculifer*.

3.2. Mg/Ca and Sr/Ca

For *G. ruber*, values for Mg/Ca are normally distributed (supporting information Figure S4 and Table S4). Standard deviations for Mg/Ca for each transect vary between 11 and 21% (supporting information Figure S4 and Table 2). The Sr/Ca results are also normally distributed for all transects and standard deviations vary between 4.5 and 13.5% (supporting information Figure S5 and Tables 2 and S4). Single-spot measurements for *G. sacculifer* showed that Mg/Ca values are normally distributed for all transects with standard deviations varying from 9 to 17% (supporting information Figure S7 and Tables 2 and S5). Values for Sr/Ca are normally distributed as well, with standard deviations varying between 4 and 13% (supporting information Figure S8 and Tables 2 and S5). Despite the positive results for PP9 Sr/Ca values for the Shapiro-Wilk test, the distribution looks randomly instead of normally distributed.

The correlation between temperature and Mg/Ca is not significant for either species when excluding the northernmost transect ($r^2 = 0.12$ and $p = 0.1$ for *G. ruber* and $r^2 = 0.80$ and $p = 0.15$ for *G. sacculifer*) (Figures 4 and 5). However, this correlation is significant for both species when including the northernmost transect ($r^2 = 0.38$ and $p < 0.001$ for *G. ruber* and $r^2 = 0.84$ and $p < 0.001$ for *G. sacculifer*) due to the considerably lower Mg/Ca for specimens from the northernmost section of the Red Sea, especially for *G. sacculifer*. Also, the correlation between salinity and Mg/Ca is not significant for either species when excluding PP9 ($r^2 = 0.15$, $p = 0.07$ for *G. ruber* and $r^2 = 0.54$, $p = 0.15$ for *G. sacculifer*) and significant when including this transect ($r^2 = 0.29$ and $p = 0.02$ for *G. ruber* and $r^2 = 0.59$ and $p < 0.001$ for *G. sacculifer*). A significant negative correlation with salinity was found for Sr/Ca, again with deviating values for the northernmost station ($r^2 = 0.90$, $p < 0.001$ for *G. ruber* and $r^2 = 0.53$, $p < 0.001$ for *G. sacculifer* excluding PP9, and $r^2 = 0.25$ and $p < 0.001$ for *G. ruber* and $r^2 = 0.53$ and $p < 0.001$ for *G. sacculifer* including PP9 (Figures 4 and 5)). With increasing temperatures, Sr/Ca values increase, except for the northernmost transect ($r^2 = 0.86$, $p < 0.001$ for *G. ruber* and $r^2 = 0.34$, $p < 0.001$ for *G. sacculifer* without PP9, and $r^2 = 0.06$ and $p = 0.09$ for *G. ruber* and $r^2 = 0.02$ and $p = 0.93$ for *G. sacculifer* including PP9). The correlation between carbonate ion content (CO_3^{2-}) and Mg/Ca is not significant for either species, whether the northernmost transect is included or excluded ($r^2 = 0.02$ and $p = 0.54$ for *G. ruber* and $r^2 = 0.25$ and $p = 0.006$ for *G. sacculifer* excluding PP9 and $r^2 = 0.04$ and $p = 0.24$ for *G. ruber* and $r^2 = 0.13$ and $p = 0.06$ for *G. sacculifer* including PP9). A significant negative correlation is observed between Sr/Ca and CO_3^{2-} for both scenarios and both species ($r^2 = 0.94$,

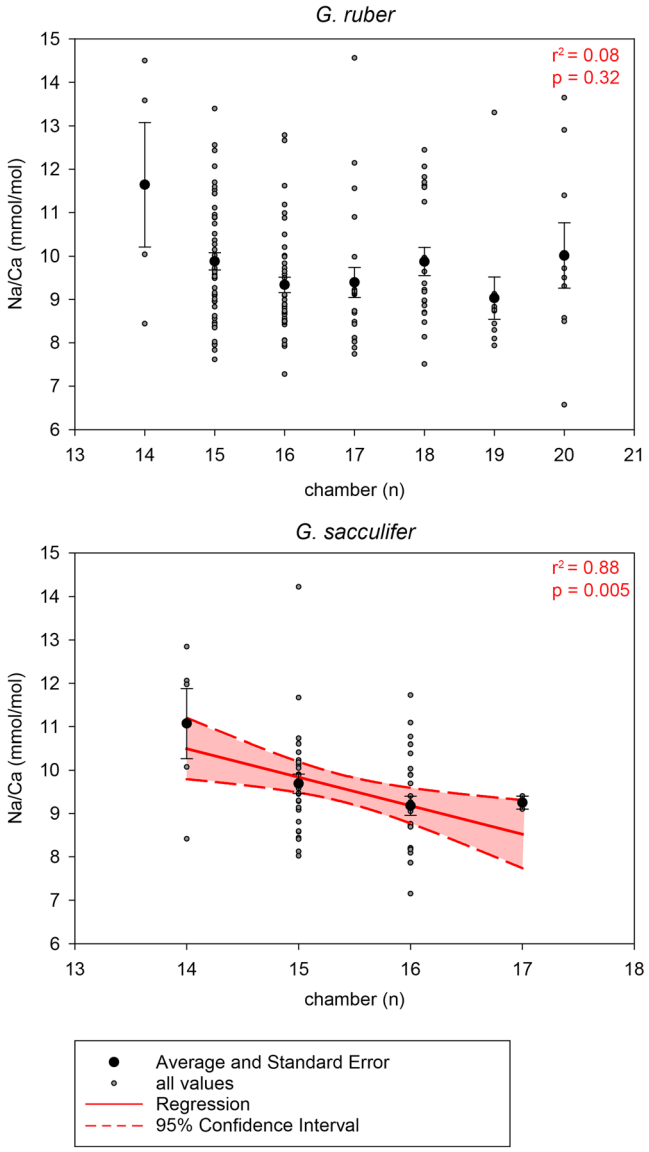

Figure 6. Na/Ca values for *G. ruber* and *G. sacculifer*, plotted against chamber number, with 95% confidence interval. The chamber number is calculated based on the measured shell diameter [*Hemleben and Bijma,* 1994; *Brummer et al.*, 1987].

$p < 0.001$ for *G. ruber* and $r^2 = 0.64$, $p < 0.001$ for *G. sacculifer* without PP9, and $r^2 = 0.55$ and $p < 0.001$ for *G. ruber* and $r^2 = 0.34$ and $p < 0.001$ for *G. sacculifer* including PP9).

3.3. Foraminiferal Shell Diameter

Only Na/Ca, Mg/Ca, and Sr/Ca in specimens from the size fraction >75 μm were analyzed, but those from the larger end of the size spectrum were more often selected for LA-ICP-MS analyses. The diameter of these specimens varies from 129 to 353 μm for *G. ruber* and from 126 to 486 μm for *G. sacculifer*. Within transects, there is no correlation between size and Na/Ca. The number of chambers for *G. sacculifer* ranges from $n = 14$ to $n = 17$ [*Hemleben and Bijma,* 1994] and for *G. ruber* between $n = 14$ and $n = 20$ [*Brummer et al.*, 1987]. When comparing chamber numbers to the measured Na/Ca values, a negative correlation is found for *G. sacculifer* (Figure 6, $r^2 = 0.88$, $p = 0.005$) and no correlation is present in Na/Ca versus chamber number in *G. ruber*. For the northernmost station (PP9), diameters are considerably larger for both species when compared to those of the other transects (Figure 7). Combining all transects except the northernmost transect, a negative and significant correlation between salinity and size was observed ($r^2 = 0.61$, $p < 0.001$ for *G. ruber* and $r^2 = 0.99$, $p < 0.001$ for *G. sacculifer*). Including the northernmost transects does not result in a significant correlation between size and salinity ($r^2 = 0.06$, $p = 0.8$ for *G. ruber* and $r^2 = 0.0003$, $p = 0.92$ for *G. sacculifer*).

4. Discussion

Currently, few Na/Ca values are reported for planktonic foraminifera to compare our data to, but overall values correspond well to those reported before for *G. sacculifer* [*Delaney et al.*, 1985; *Allen et al.*, 2016], *G. ruber* (pink) [*Allen et al.*, 2016] and the benthic foraminiferal species *Ammonia tepida* [*Wit et al.*, 2013], albeit with an offset toward higher absolute values. Both planktonic foraminifera and *A. tepida* are known to build shells relatively low in minor and trace elements compared to the composition of large benthic foraminifera [*Lea et al.*, 1999; *Munsel et al.*, 2010]. Measured Mg/Ca and Sr/Ca are similar to values reported previously for *G. ruber* and *G. sacculifer* (e.g., from a sediment trap study reporting values for 10 planktonic species in *Anand et al.* [2003], *Fallet et al.* [2010], *Hönisch et al.* [2013], *Kısakürek et al.* [2008], and *Steinhardt et al.* [2014]).

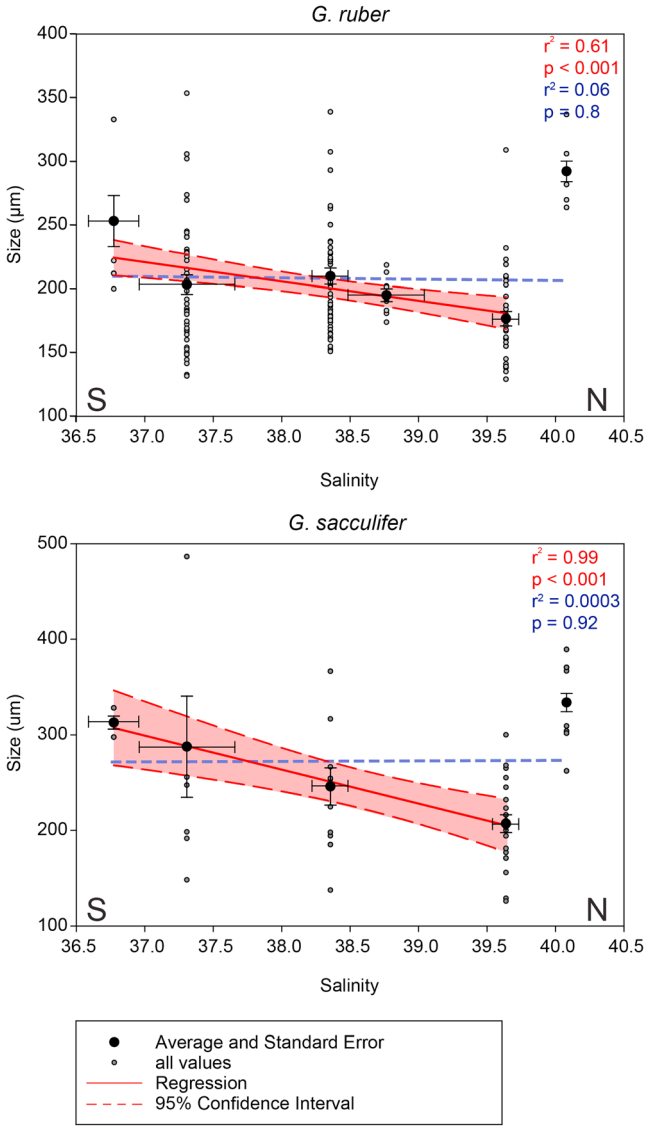

Figure 7. Salinity (transects) versus size for *G. ruber* and *G. sacculifer*; r^2 was calculated using weighted average size values per salinity. Horizontal error bars for salinity indicate values at the start and end of each transect. The dotted (light blue) trend lines show the non-significant correlations between salinity and size, when including the northernmost transect.

4.1. Na/Ca

4.1.1. Comparison to Previous Calibrations

The Na/Ca values of calcite of living planktonic *G. ruber* specimens from the Red Sea show a clear positive and significant linear correlation with salinity ($Na/Ca = 0.66 \times S - 15.75$, $r^2 = 0.88$, $p < 0.001$), which is insignificant for *G. sacculifer* ($Na/Ca = 0.229 \times S + 0.67$, $r^2 = 0.19$, $p = 0.11$) (Figure 3). Laser ablation analyses, although also adding to the number of analyses needed per transect, allow identifying intraspecimen and interspecimen variability. In contrast to solution SF-ICP-MS, measurements can be performed on individual specimens and chambers, allowing investigating natural variability. In case Na would be adsorbed or absorbed to the calcite shell surface, this is also obvious from ablation profiles. In such cases, part of the profile with elevated trace or minor element/Ca ratios were discarded and therefore do not bias the analysis. However, only minor surface contamination was observed, in conjunction with Al in some specimens. Hence, Na contamination can be ruled out as a factor causing variability in Na/Ca within and between specimens and species. Due to the small shell size of these foraminifera, we were not able to perform sufficient duplicate measurements on single chambers to allow robust statistical testing of intra chamber variability. However, variability in Na/Ca values between chambers was up to 14%, which is comparable to or smaller than that observed for Mg/Ca in other studies using LA-(Q)-ICP-MS [e.g., *Dueñas-Bohórquez et al.*, 2009; *De Nooijer et al.*, 2014a]. So far, there is no consensus on the cause of this small-scale variability in composition for other elements. Environmental variability cannot account for (all) element variability between single-chamber analyses. Possibly, the same process responsible for small-scale heterogeneity (i.e., banding) in Mg/Ca [e.g., *Eggins et al.*, 2004] could also partially explain the observed scatter in Na. Since the calcite precipitated during each chamber addition also envelops the rest of the foraminiferal shell, higher Na concentrations associated with earlier stages of chamber addition could offset element/Ca ratios between chambers. In this case small changes in thickness of these bands could affect elemental ratios measured at a single-spot or between chambers due to the nature of foraminifera to add chambers. However, within the ablation profiles no evidence for such banding was observed and studies specifically addressing the microscale distribution in a smaller scale than laser ablation of Na in a calcite foraminifer shell are necessary to understand the potential role of the observed small-scale variability in element/Ca ratios.

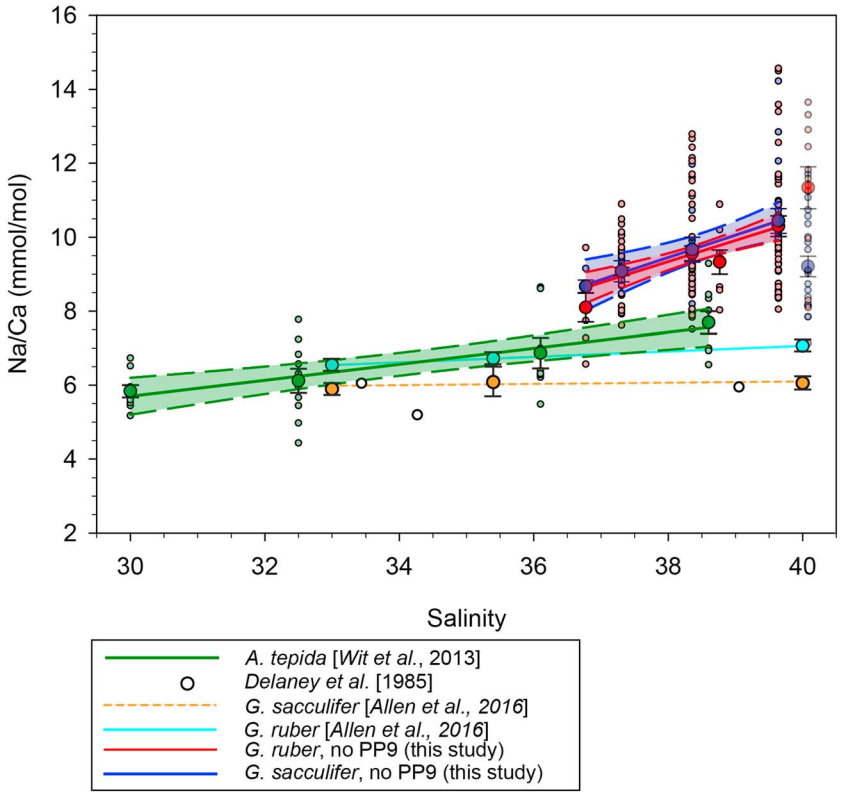

Figure 8. Our Na/Ca data for *G. sacculifer* and *G. ruber*, compared to the benthic species *Ammonia tepida* from culturing ($Na/Ca = 0.22 \times S - 0.75$ [*Wit et al.*, 2013]), values from culture experiments for *G. sacculifer* from *Delaney et al.* [1985] and culture study results for *G. ruber* (pink) and *G. sacculifer* from *Allen et al.* [2016]. Averages (large dots), standard errors, linear regressions (straight lines), and the 95% confidence interval (shaded areas) are also indicated. The error bars of *Allen et al.* [2016] are based on the largest % difference among three consistency standards or the 1σ of replicate measurements.

Foraminiferal sizes do not correlate with measured Na/Ca ratios in this study. However, for *G. sacculifer* calculated chamber numbers do show a correlation with Na/Ca ratios (Figure 6). The apparent correlation between Na/Ca ratios and chamber position suggests that chamber position, rather than absolute size, might influence Na incorporation. However, even though a significant negative trend is observed between chamber number and Na/Ca, many other factors covary as well along the Red Sea (e.g., salinity, temperature, and CO_3^{2-}). Also, although *Wit et al.* [2013] did show a correlation between size and Na/Ca for *A. tepida*, they argued that this correlation is spurious. Since final size of the cultured foraminifera changed with salinity, it was argued that this was an indirect relation, with salinity being the main contributor to the observed trend in size versus Na/Ca. This observation may also explain the trend in Na/Ca with chamber number in our data set. As all our specimens were collected from surface waters using a plankton pump, we can exclude such trends related to gradual changes with water depth during foraminiferal life (ontogenetic vertical migration).

Comparing the Na/Ca-salinity relationship of both planktonic species with the previously reported benthic species, *A. tepida* [*Wit et al.*, 2013] shows a positive response of Na incorporation for all species with salinity (Figure 8), albeit that the sensitivity reported here is higher for the planktonic than for the benthic species. For the culture study with *Globigerinoides ruber* (pink) and *G. sacculifer* of *Allen et al.* [2016], as well as the benthic *A. tepida* [*Wit et al.*, 2013], the correlations of this study show a slight offset toward higher absolute values and a significantly steeper slope (one-way analysis of covariance, $p < 0.5$) (Figure 8). Also, *Allen et al.* [2016] found that only the relation between salinity and Na/Ca for *G. ruber* is significant although different absolute values for *G. ruber* and *G. sacculifer* were measured. Potential explanations for the observed offset between these studies include (1) the limited overlap of salinity intervals studied in these studies and with the benthic *A. tepida*, (2) different biomineralization controls or life stage, or (3) an effect of carbonate chemistry and temperature in the field-collected specimens.

First, there is only limited overlap in salinity intervals between this study (from 36.8 to 40.1 in this study and from 30.0 to 38.6 in *Wit et al*. [2013]). This complicates comparing responses to salinity (Figure 8). However, recent culture results on the same species suggest that this proxy for *G. ruber* can be extended to a salinity of 33 [*Allen et al*., 2016], albeit with a less steep slope.

Second, partition coefficients (D_{Na} = Na/$Ca_{foraminifer}$/Na/$Ca_{seawater}$ in mmol/mol) of this study (D_{Na} = 0.18–0.25×10^{-3}) are slightly higher than for *Wit et al*. [2013] (D_{Na} = 0.12–0.16×10^{-3}) and *Allen et al*. [2016] ($D_{Na} = 0.1 \times 10^{-3}$), but comparable to inorganic precipitation experiments (0.07–$0.20 \times 10 - 3$) [*Kitano et al*., 1975; *Ishikawa and Ichikuni*, 1984, *Okumura and Kitano*, 1986], suggesting no major impact of biology. However, although the two planktonic species here are comparable in their calibration (up to a salinity of ~39.6, Figure 3), we do observe a difference with results presented by *Allen et al*. [2016]. This difference between our field-collected *G. ruber* and *G. sacculifer* and their cultured specimens may be caused by additional controls in the field environment (e.g., the effect of a particular combination of salinity, temperature, and carbonate chemistry in the Red Sea), which is discussed later in this section, or a difference in size/life stage [e.g., *Anand et al*., 2003]. At different foraminiferal developmental stages, also the partitioning of elements from seawater to calcite could change [e.g., *Dueñas-Bohórquez et al*., 2011]. Furthermore, terminal calcification features (e.g., cortex or crust) for many planktonic species are found to have a different structure and thickness and differ in Mg and probably also other elements [e.g., *Nürnberg et al*., 1996; *Steinhardt et al*., 2015]. Also, when applying a linear correlation for the combined planktonic species of this study, the extrapolated calibration intersects the *Y* axis (i.e., at a foraminiferal Na/Ca of 0 mmol/mol) at a salinity of 20.7, implying that Na/Ca decreases more strongly with salinity below ~36.5. Extrapolating the correlation from the benthic foraminiferal culturing study [*Wit et al*., 2013], results in a zero *Y* axis intercept at a salinity approximating zero, suggesting that incorporation of Na as a function of salinity follows a linear trend over a large salinity range and, moreover, is consistent with inorganic precipitation experiments [*Kitano et al*., 1975; *Ishikawa and Ichikuni*, 1984]. The observed offset between species and between benthic and planktonic foraminifera from this study might be caused by differences in biomineralization controls. Possibly, Na incorporation in benthic foraminifera resembles inorganic partitioning, whereas biomineralization in planktonic species is offset by a process responsible for a slight enrichment in Na during chamber formation. However, this contradicts with the study by *Allen et al*. [2016] for the same planktonic species, in which the absolute values are similar to *A. tepida* [*Wit et al*., 2013]. Also, the presence of symbionts in the studied planktonic species, in contrast to the benthic *A. tepida* studied by *Wit et al*. [2013] might affect Na partitioning. Photosynthesis by foraminiferal symbionts influences uptake of inorganic carbonate species, thereby potentially enhancing calcification and affecting element incorporation [*Rink et al*., 1998, *Köhler-Rink and Kühl*, 2005; *De Nooijer et al*., 2014b]. This does not, however, explain the difference between our results and those of *Allen et al*. [2016].

The most probable explanation for the different Na/Ca calibrations between our results and those from previous studies is that the Red Sea has many covarying factors and an unusual environmental setting compared to those applied in culturing studies. Also, several parameters from the sea water carbonate system (calcite saturation state (Ω), DIC, and alkalinity) from the Red Sea differ markedly from the open ocean, since these factors increase with increasing salinities [e.g., *Sarmiento and Gruber*, 2006], favoring calcium carbonate shell precipitation and possibly enhance incorporation of Na and other elements as a result of enhanced growth rates. Although observed trends in Na incorporation can be fully explained using changes in Na and Ca activities [*Wit et al*., 2013], a (minor) role of carbonate chemistry cannot be fully excluded. Recent culture results suggest a positive trend in Na/Ca values with increasing [CO_3^{2-}] [*Allen et al*., 2016], which is opposite of the trend observed here. Still, the range in carbonate ion concentrations sampled here is relatively limited. Comparing the carbonate ion content in the study of *Wit et al*. [2013], on average 246.5 μmol/kg seawater, which is much higher than that of the Red Sea (219.5 μmol/kg seawater), would imply a stronger impact on the benthic foraminiferal values, which is not observed here. Temperature may also have an effect on Na incorporation. Recent culture results using the same two planktonic species cultured in different temperatures, carbonate chemistry, and salinities suggest that temperature has a negative effect on Na/Ca values [*Allen et al*., 2016]. The negative trend suggested by *Allen et al*. [2016] between temperature and Na/Ca might have resulted in a slightly steeper slope compared to the *Wit et al*. [2013] data and *Allen et al*. [2016], but this offset is not enough to explain the overall observed difference. Moreover, the only significant correlation between environmental variables

and Na/Ca in cultured planktonic foraminifera [*Allen et al*., 2016] was with salinity, which is in line with *Wit et al.* [2013].

Still, because of the many covarying factors compared to culture experiments, it remains challenging to fully compensate for all potential additional effects in a natural environment like the Red Sea. The correlations suggested between Na/Ca values, temperature, and carbonate ion content are more likely the consequence of environmentally covarying factors (e.g., carbonate chemistry and salinity) (Figure 3).

4.1.2. Na/Ca in *G. ruber* versus *G. sacculifer*

Results show a significant positive correlation between Na/Ca and salinities for *G. ruber*, but not for *G. sacculifer* (Figure 3). This is similar to the results found by *Allen et al.* [2016], also showing that only Na/Ca in *G. ruber* has a significant positive correlation with salinity. The observed difference between these two species could be due to Na/Ca for *G. sacculifer* simply not being correlated to salinity or to a larger uncertainty in the regression in the *Allen et al.* [2016] study. Also clearly visible is the fact that average Na/Ca values in foraminifera from the northernmost transect for *G. sacculifer* strongly deviate from the observed overall trend and from the trend observed for *G. ruber*. This offset in the northernmost location is observed not only for Na/Ca but also for Mg/Ca and Sr/Ca, as well as shell size for both species studied. In addition, at this transect the distribution of element concentrations also displays slightly more variability and/or clustering into two groups, especially for the Na/Ca in *G. ruber* and Sr/Ca in *G. sacculifer* (Figures 3–5, 7, S3, and S8). The overall difference of the last transect suggests that the foraminifera sampled are somehow not representative for the environment they were collected from. Possible explanations for these deviating values and distribution of element concentrations in the northernmost transect are the following: (1) postmortem inorganic overgrowths [*Hoogakker et al*., 2009] and/or (2) advection of an expatriate population/specimens [*Auras-Schudnagies et al*., 1989] and/or (3) prevalence of specimens with a different life stage in this area and/or (4) high temporal or spatial environmental variability in this part of the Red Sea.

Inorganic overgrowths are known to affect elemental ratios measured on foraminifera from core top material [*Hoogakker et al*., 2009]. However, since all foraminifera were collected from surface waters using plankton pumping, diagenesis can be ruled out as a potential source for the observed offset. Upon collection samples were directly washed and stored to minimize potential impacts on the foraminiferal calcite elemental composition after sample collection (see section 2). Hence, the reported Na/Ca, Mg/Ca, and Sr/Ca represent the primary signal as precipitated by the foraminifera while still living.

Second, the difference in (monsoonal) intensity, source, and distribution of surface water currents, as already found by *Auras-Schudnagies et al.* [1989], or exchange with another water mass might explain the distribution of species in an area. Using stable oxygen isotopes, *Auras-Schudnagies et al.* [1989] discovered that the species *Globorotalia menardii* survives transport from the south to the north of the Red Sea but stops calcifying during this journey. If this were also true for *G. ruber* and *G. sacculifer*, this would also explain the larger sizes in the northernmost transect, corresponding to the larger sized foraminifera in the southernmost transect. Also, the lower Na/Ca values and Mg/Ca values in the northernmost transect would respectively indicate lower salinities and colder temperatures from the southern Red Sea. The change in monsoonal strength between summer and winter does not affect salinities noticeably (World Ocean Atlas (WOA) 2001) [*Boyer et al*., 2005] and maximum temperatures only become ~2°C lower at the southernmost position [*Boyer et al*., 2005]. Therefore, the deviating values could not be fully explained by a change in monsoonal strength. Moreover, one would expect similar effects in all of the transects in between, which is not observed.

Another, and to our opinion more probable source for expatriates, involves inflow from the less saline Mediterranean, which would introduce an anti-Lessepsian population into this area. Such a population would be influenced by geochemical signals recorded in the Suez Canal (with salinities of to 45) and/or the eastern Mediterranean (S = ~20.8, T = ~38.9, WOA01 [*Boyer et al*. 2005]). Even though transport through the Suez Canal is found to be mostly from south to north [e.g., *Por*, 2012], the flow through the Bitter Lakes does change its flow direction from July to September [*Biton*, 2015]. This is confirmed using ocean modeling and environmental observations [e.g., *Golani*, 1998]. The presence of two living *G. ruber* (pink) specimens in our northernmost sample also suggests inflow from north to south. This species has not been observed in the Red Sea area since 120,000 years B.P. [*Thompson et al*., 1979] but is still common in the Mediterranean. Being expatriated from the Mediterranean, these foraminifera would also (partially) be affected by lower salinities and temperatures, which is in line with the observed lower Na/Ca and Mg/Ca

values (Figures 3–5). Furthermore, temperatures decrease very sharply northward of the last sampled transect, compared to the rest of the Red Sea (Figure 1b), potentially indicating inflow from colder Mediterranean Sea water. The overall larger shell sizes found in the northernmost transect also suggest a later moment in ontogeny compared to the specimens sampled on the other transects (Figure 7), which is in line with a population largely being made up of expatriates.

Third, even though the specimens analyzed here were selected based on shell size, with the larger ones being more suitable for analyses and a size fraction <75 μm not taken into account, this does not explain the overall differences in element uptake. Although the "larger" sized foraminiferal assemblage could explain part of the offset (Figures 7 and 8), the observed difference is much larger. Moreover, not all elements showing contrasting elemental ratios are also correlated to shell size. Hence, shell size alone cannot explain the observed offset for the northernmost transect.

Fourth, it is unlikely that all specimens collected at the northernmost transect derive from a specific event such as upwelling or a local rainfall and freshwater event, since upwelling typically occurs in the southern Red Sea and rainfall is extremely low in this area (3 mm/yr) [*Zahran*, 2010]. Still, since the population of analyzed foraminifera for each transect was collected over a distance of approximately 225 km and foraminiferal densities (specimens per liter seawater) were not necessarily evenly distributed along these transects, element ratios might be biased toward specific intervals. Short-lived events and or local phenomena might hence be disproportionally represented. A detailed temperature record obtained during the cruise (Figure 1b) shows that at least temperature increased gradually over the transect (Figure 1). Salinities within this transect vary no more than 0.02 units, which would only explain an offset of 0.01 mmol/mol in Na/Ca, based on the calibration in Figure 3.

The deviating sizes, Mg/Ca, Sr/Ca, and Na/Ca values of the foraminifera at the northernmost transect, in conjunction with the observation of living *G. ruber* (pink) specimens, indicating inflow from the colder, less saline Mediterranean, argue for excluding the northernmost transect from the calibrations. This results in similar, positive, and significant correlations for both planktonic species, respectively, Na/Ca (mmol/mol) = 0.57 × S–12.38 ($r^2 = 0.91$, $p < 0.001$) for *G. ruber* and Na/Ca = 0.60 × S–13.49 ($r^2 = 0.999$, $p < 0.001$) for *G. sacculifer*.

4.2. Mg/Ca and Sr/Ca

Values for Mg/Ca of *G. ruber* closely correspond to those given by *Kısakürek et al.* [2008] and are somewhat lower than in the sediment trap study (for 10 planktonic species) by *Anand et al.* [2003]. For the reported salinities, *G. ruber* Mg/Ca values are comparable to *Hönisch et al.* [2013] and *Kısakürek et al.* [2008]. *Globigerinoides sacculifer* shows somewhat lower Mg/Ca values compared to *G. ruber*, which is in line with previous observations [*Anand et al.*, 2003; *Nürnberg et al.*, 1996]. For the measured temperatures and salinities, Mg/Ca values of *G. sacculifer* are somewhat lower than that measured by *Nürnberg et al.* [1996], *Anand et al.* [2003], *Hönisch et al.* [2013], and *Dueñas-Bohórquez et al.* [2009]. In our data set, Mg/Ca values for both species are significantly positive correlated to temperature and negative to salinity. For reasons mentioned in section 4.1.2, we think that specimens collected at the northernmost transect might not be representative for the environment they were collected in. When excluding this transect from the regressions, this results in nonsignificant correlations between Mg/Ca and temperature as well as salinity for both species. As salinity and temperature both positively affect foraminiferal Mg/Ca [e.g., *Dueñas-Bohórquez et al.*, 2009; *Anand et al.*, 2003; *Wit et al.*, 2013] and are inversely correlated in the Red Sea, their influence on the specimens measured here counteract the incorporation of Mg. Even though the relative impact of salinity on Mg/Ca is small (respectively 0.11 mmol/mol per salinity unit [*Dueñas-Bohórquez et al.*, 2009, and references therein], 0.15 mmol/mol per salinity unit [*Hönisch et al.*, 2013], and 0.16 mmol/mol per salinity unit [*Kısakürek et al.*, 2008]), this could explain the absence of a significant correlation between temperature and Mg/Ca in our data set when excluding PP9. Accordingly, when applying species-specific salinity corrections for a salinity of 35 on the Mg/Ca ratios, the calibrations between temperature and Mg/Ca ratios become steeper and also (more) significant, also when including the northernmost transect (respectively $r^2 = 0.51$ and $p < 0.001$ for *G. ruber* and $r^2 = 0.88$ and $p < 0.001$ for *G. sacculifer* without PP9 and $r^2 = 0.69$ and $p < 0.001$ for *G. ruber* and $r^2 = 0.96$ and $p < 0.001$ for *G. sacculifer* with PP9) [*Kısakürek et al.*, 2008; *Hönisch et al.*, 2013] (Figure 9). In total, Mg/Ca values after the salinity corrections decreased by 9% (south) to 31% (north) for *G. ruber* and by 8.5% (south) to 34.5% (north) for *G. sacculifer*. This implies that although Mg/Ca values in the sediment are not well connected to temperature [*Hoogakker et al.*, 2009], surface water temperatures are well registered by foraminiferal Mg/Ca values.

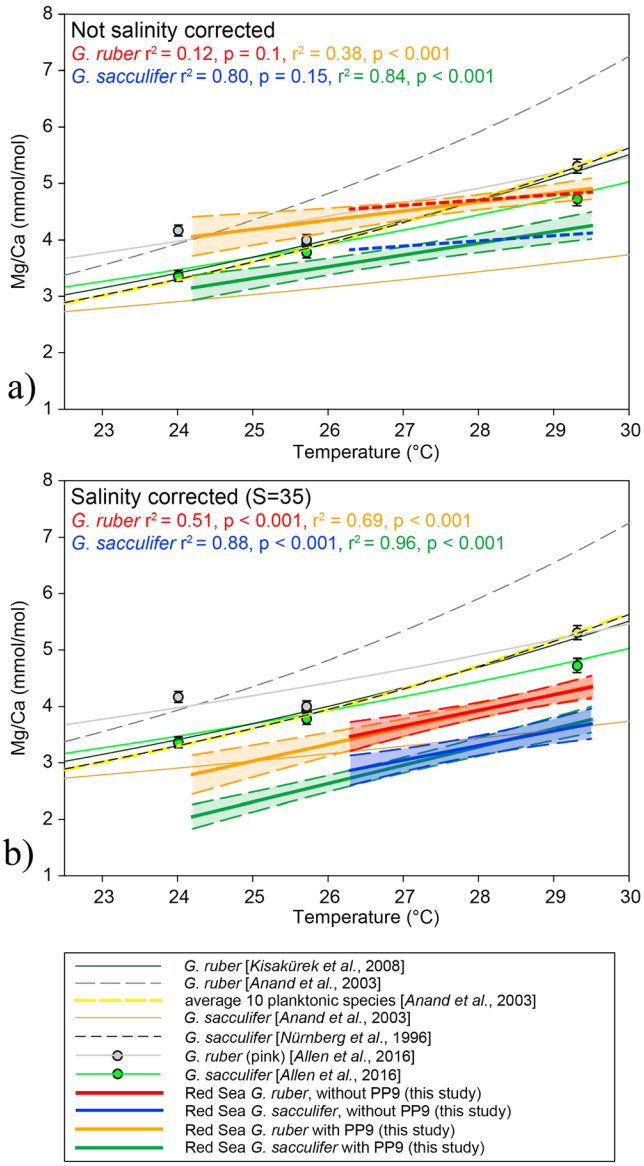

Figure 9. Calibrations of (a) non salinity-corrected Mg/Ca values and (b) salinity-corrected Mg/Ca values for a salinity of 35 based on the calibrations of *Kısakürek et al.* [2008] for *G. ruber* and *Hönisch et al.* [2013] for *G. sacculifer*, with their 95% confidence intervals. Horizontal error bars indicate temperatures recorded at the start and end of each transect. The vertical error bars are the standard errors of the mean, except for the *Allen et al.* [2016] data, where they represent the long-term relative standard deviation. Calibrations from other studies are also added [*Kısakürek et al.*, 2008; *Anand et al.*, 2003; *Nürnberg et al.*, 1996; *Allen et al.*, 2016].

Also, size could have an effect on the Mg/Ca, as well as on the Sr/Ca ratio. It was found by *Elderfield et al.* [2002] that Mg/Ca increases with size whereas Sr/Ca decreases with size for both *G. ruber* and *G. sacculifer*. However, this would only account for a maximum Mg/Ca difference of 0.49 mmol/mol for *G. ruber* and 0.16 mmol/mol for *G. sacculifer* in the size ranges measured in this study. Since sizes decrease toward the north as well as temperatures and Mg/Ca values, one would expect the size effect to result in a steeper relation adding to the correlation with temperature, which is not the case. Hence, we refrained from correcting for size here.

According to *Steinke et al.* [2005], morphotypes could influence the Mg/Ca composition with ~0.37 mmol/mol difference between the *G. ruber* in a strict sense (sensu stricto) and in a broad sense (sensu lato) morphotype. We were not able to distinguish between morphotypes among *G. ruber* in our samples as distinctive morphological traits are restricted to terminal (reproductive) stages typically found in sediments, while our samples are from a growing population of late neanic to late adult (nonreproductive) stages [*Brummer et al.*, 1987]. However, as also suggested by *Steinke et al.* [2005], either depth habitat or seasonality plays a role in the distribution of these subspecies. The *G. ruber* in a strict sense morphotype records higher temperatures (Mg/Ca and $\delta^{18}O$) than *G. ruber* in a broad sense. Since the in a strict sense morphotype is identified to dwell in the upper 30 m of the water column and the in a broad sense morphotype at greater depths [*Wang*, 2000], our surface water specimens most likely mainly consists of the *G. ruber* in a strict sense morphotype. Therefore, it is very unlikely that different morphotypes influenced our data.

Obtained Sr/Ca values are similar or somewhat higher compared to those reported in previous studies [*Lea et al.*, 1999, *Dissard et al.*, 2010; *Wit et al.*, 2013; *Dueñas-Bohórquez et al.*, 2009; *Kısakürek et al.*, 2008; *Russell et al.*, 2004]. However, the observed negative trend with salinity, both with and without the northernmost transect, differs remarkably from other studies, previously suggesting a (sometimes slightly) positive correlation [*Dissard et al.*, 2010; *Wit et al.*, 2013; *Dueñas-Bohórquez et al.*, 2009, *Lea et al.*, 1999, *Kısakürek et al.*, 2008]. This implies that other factors along the Red Sea from south to north must somehow override an impact of salinity on Sr incorporation. Other potential known impacts for Sr incorporation are (1) sea water carbonate

chemistry, (2) temperature, salinity, and size, (3) sea water Sr/Ca values, and (4) sea water Ca to carbonate ion stoichiometry.

First, carbonate chemistry (dissolved inorganic carbon (DIC) and total alkalinity (TA)) is found in controlled growth experiments to affect Sr incorporation positively with higher TA or DIC values [*Dissard et al*., 2010; *Dueñas-Bohórquez et al*., 2009]. In general, with increasing salinities, DIC and seawater alkalinity also increase [*Sarmiento and Gruber*, 2006] and thus higher DIC, alkalinity, and related carbonate ion values are found in the north (Table 1). This would therefore result in increased Sr incorporation toward the north, which is opposite to the observed negative correlation.

Second, temperature has been suggested to impact foraminiferal Sr/Ca values as well [*Kısakürek et al*., 2008; *Lea et al*., 1999]. The incorporation of Sr was shown to increase with increasing temperatures, with a slope for *G. ruber* of $\Delta(\mathrm{Sr/Ca})/\Delta T = 0.01$ mmol/mol/°C [*Kısakürek et al*., 2008]. The difference in temperature from south to north is 5.3°C, which would result in a decrease of 0.053 mmol/mol Sr/Ca (and without northernmost transect 4.2°C, resulting in a difference of 0.042 mmol/mol). The difference in temperature across the Red Sea could hence account for not more than 10% of the observed decrease in Sr values toward the northern Red Sea. Also, salinity has been suggested to have a small impact on Sr/Ca ratios, with an increase of 0.008 mmol/mol Sr per °C [Dueñas-Bohórquez *et al*., 2009, and references therein]. However, an opposite trend is observed between salinity and Sr/Ca in these samples, suggesting an overriding effect of another variable on the incorporation of Sr. The difference in salinity between south and north is 3.3, which would only account for an increase of 0.03 mmol/mol Sr/Ca from south to north. The effect of size on Sr/Ca is negligible: within the size range measured in this study, the Sr/Ca ratio could differ 0.02 mmol/mol for *G. ruber* and 0.03 mmol/mol for *G. sacculifer* [*Elderfield et al*., 2002].

Third, even though Sr is considered to be a conservative element in seawater (residence time 4.9×10^6 years), changes in Sr/Ca values are observed in both depth profiles as well as in aging surface waters. Acantharians, abundant marine planktonic protists, incorporate Sr into their skeletons and cysts in the form of celestite ($SrSO_4$), thereby transporting Sr from the sea surface toward deeper layers of the ocean and/or seas where Sr is enriched through the subsequent remineralization/dissolution of these frustules [*Bernstein et al*., 1987; *North*, 1974; *Odum*, 1951; *Hurd and Spencer*, 1991]. The Sr concentration in the Red Sea surface seawaters could thus gradually deplete in Sr as it slowly flows from Bab el Mandeb toward the north. *De Deckker* [2004] calculated that with a hypothetical 10 specimens per liter, up to 7.6 μg of Sr would be taken up in one generation of acantharids. For the Red Sea, assuming two generations per year and a residence time of Red Sea water of 36 years, this would remove up to ~547 μg/L [*Cember*, 1988; *De Deckker*, 2004] and hence result in an ~7% offset in Sr concentrations. With a constant D_{Sr} this would result in gradually lower foraminiferal Sr/Ca values, with similar amplitude as observed. A potential temperature effect could thus be enhanced by a gradual Sr depletion toward the north. Still, no actual proof exists for such offsets being present in Red Sea surface water and a role of acantharians therein.

Fourth, also, the calcium to bicarbonate ratio is known to affect Sr incorporation [*Nehrke et al*., 2007]. The $[Ca^{2+}]$:$[CO_3^{2-}]$ stoichiometry is known to affect growth rate of calcite [*Nehrke et al*., 2007], with highest growth rates for a $Ca{:}CO_3^{2-}$ ratio close to 1. Growth rates, on the other hand, influence the partition coefficient of Sr into calcite positively. However, one would not expect this ratio to change significantly in sea water as both Ca and carbonate ion concentration are intimately tied through carbonate production. Either way, the negative correlation between salinity and foraminiferal Sr/Ca is sufficiently significant in the Red Sea to warrant further investigation.

4.3. Sodium as a Direct Proxy for Salinity and Future Application

Even though Na/Ca values of calcite of living planktonic species from the Red Sea show a promising significant linear correlation with salinity for either both species (*G. sacculifer* and *G. ruber*) or only *G. ruber*, several issues need further research. Since the plankton pump samples are collected over intervals of approximately 225 km along which foraminiferal densities most likely varied, specimens analyzed might not have produced their shells at the average recorded salinity of that transect (Figure 1). An offset from the average salinity toward the minimum or maximum salinity of a transect could account for at most a 0.62 mmol/mol offset in Na/Ca within a transect (PP2: difference minimum and maximum salinity is 1.15). Most transects cover much less change in salinity, varying from 0.02 to 0.5 between the minimum and maximum salinity, and could account for at most 0.27 mmol/mol of the observed Na/Ca ranges. Additional controlled growth

experiments isolating individual parameters are necessary to reduce uncertainties in planktonic Na/Ca and potentially reconcile observed differences between cultured and field-derived calibrations. Furthermore, for the wider applicability of this proxy, it is necessary to test whether the correlation, and offset with the earlier reported calibration, is specific to the Red Sea area. *Bijma et al.* [1990a] showed that *G. sacculifer* grows between salinities of 19–48 and *G. ruber* between 19 and 50, making an extension of the salinity range for this Na/Ca-salinity proxy theoretically possible. Recent results from a culture study for the same species [*Allen et al*., 2016] show that a relationship to salinity for *G. ruber* holds down to salinities of 33. Extrapolation to the natural environment would need to be verified using samples from outside the Red Sea.

The large intraspecimen and interspecimen variability is currently limiting the precision of Na-based salinity reconstructions. The observed variability in Na/Ca between individuals and/or foraminiferal shell chambers might be considerable but is in line with previous studies using single-spot foraminiferal shell analyses [e.g., *Reichart et al*., 2003; *Wit et al*., 2013; *Dueñas-Bohórquez et al*., 2009; *Dissard et al*., 2010; *De Nooijer et al*., 2014a; *Sadekov et al*., 2008]. The uncertainty in reconstructed salinities associated with the here established Na/Ca to salinity calibration is still considerable at ~0.8 and ~1.2 for *G. ruber* and *G. sacculifer*, respectively (95% confidence intervals of calibration in central part of the calibration). This uncertainty does not affect reconstructed relative changes, which would mainly suffer from uncertainties in Na/Ca values at a specific interval. The standard errors of the averages are relatively low due to the number of specimens measured in this study. By increasing the number of specimens analyzed, the precision (not accuracy) of these reconstructions improves considerably. Based on the measured SD, the amount of specimens needed for estimating past salinity better than 0.1 unit (SE = ~0.05 mmol/mol) is between 14 and 37 for *G. ruber* and between 7 and 28 for *G. sacculifer* (supporting information Figure S9). Within the open ocean salinity variations are, however, small and other analytical approaches and or calibrations would be necessary. However, application of Na/Ca to areas experiencing large salinity changes, such as more marginal settings and estuaries, is with the existing calibrations now within reach.

5. Conclusions

This study represents the first field calibration on incorporation of Na in foraminiferal calcite as a potential proxy for salinity. The Red Sea area is particularly suitable for this purpose, since it covers a broad salinity range in a steep gradient within the same water mass. Values for Na/Ca of the planktonic foraminifera *G. ruber* (white) and *G. sacculifer* collected alive from Red Sea surface waters correlate positively and significantly with salinity. Furthermore, absolute values and slopes are similar for both species. Based on (1) the deviating Na/Ca, Mg/Ca, Sr/Ca, (2) the larger size of the specimens, and (3) the occurrence of *G. ruber* (pink), it is hypothesized that specimens in the northernmost transect are likely expatriated (i.e., from the Eastern Mediterranean) and should therefore be excluded from the Na/Ca-salinity calibration. However, Na/Ca values differ significantly from previously reported values for a cultured benthic species and for the planktonic species *G. sacculifer* and *G. ruber* (pink), which may be due to differences in biomineralization controls between these groups or the additional effects of covarying environmental variables in the Red Sea. Due to the opposing gradients in salinity and temperature in the Red Sea, the absence of a correlation between Mg/Ca values and temperature is an indication of the dampening effect of salinity over temperature on the incorporation of Mg into planktonic foraminiferal calcite. As was already found for other elements in previous studies, intraspecimen and interspecimen variability in Na/Ca (as for other elements) is considerable even though the average is very accurate, which could result in relatively large uncertainties in salinity reconstructions when not measuring sufficient specimens. Future research should therefore focus on the cause(s) for the observed variability between chambers, should quantify the impact of other environmental variables on Na incorporation, include other species, and investigate Na incorporation across planktonic foraminiferal life stages. Based on this study, incorporation of Na in foraminiferal calcite appears a valuable proxy for salinity, although species-specific calibrations seem necessary.

Acknowledgments
All data supporting the conclusions in this manuscript can be obtained from the different tables in the manuscript and supporting information. We thank Bärbel Hönisch for the DIC and alkalinity data from the RV *Pelagia* cruise 64PE158 and her constructive comments. We acknowledge Katherine Allen for sharing her culture study results at an early stage. We also thank the two anonymous reviewers for their critical reading of the manuscript and comments, which substantially improved this manuscript. We are also grateful to all technical staff on board of the RV *Pelagia* cruise 64PE158 as well as Inge van Dijk and Rineke Gieles for help in producing the NIOZ house standard for foraminiferal calcite. This work is supported by the Gravitation grant NESSC from the Dutch Ministry of Education, Culture and Science.

References

Allen, K. A., B. Hönisch, S. M. Eggins, L. L. Haynes, Y. Rosenthal, and J. Yu (2016), Trace element proxies for surface ocean conditions: A synthesis of culture calibrations with planktic foraminifera, *Geochim. Cosmochim. Acta*, doi:10.1016/j.gca.2016.08.015, in press.

Anand, P., H. Elderfield and M. H. Conte (2003), Calibration of Mg/Ca thermometry in planktonic foraminifera from a sediment trap time series, *Paleoceanography*, *18*(2), 1050, doi:10.1029/2002PA000846

Auras-Schudnagies, A., D. Kroon, G. Ganssen, C. Hemleben, and J. E. van Hinte (1989), Distributional pattern of planktonic foraminifers and pteropods in surface waters and top core sediments of the Red Sea, and adjacent areas controlled by the monsoonal regime and other ecological factors, *Deep Sea Res.*, *36*(10), 1515–1533.

Barker, S., M. Greaves and H. Elderfield (2003), A study of cleaning procedures used for foraminiferal Mg/Ca paleothermometry, *Geochem. Geophys. Geosyst.*, *4*(9), 8407, doi:10.1029/2003GC000559

Bernstein, R. E., P. R. Betzer, R. A. Feely, R. H. Byrne, M. F. Lamb, and A. F. Michaels (1987), Acantharian fluxes and strontium to chlorinity ratios in the North Pacific Ocean, *Science*, *237*(4821), 1490–1494, doi:10.1126/science.237.4821.1490.

Bijma, J., W. W. Faber, and C. Hemleben (1990a), Temperature and salinity limits for growth and survival of some planktonic foraminifers in laboratory cultures, *J. Foraminiferal Res.*, *20*(2), 95–116.

Biton, E. (2015), The Suez Canal dynamic and its impacts on water mass structure in the Mediterranean Sea: A modeling study, paper presented at 26th IUGG general assembly 2015.

Boyer, T., S. Levitus, H. Garcia, R. A. Locarnini, C. Stephensand, and J. Antonov (2005), Objective analyses of annual, seasonal, and monthly temperature and salinity for the World Ocean on a 0.25 grid, *Int. J. Climatol.*, *25*(7), 931–945, doi:10.1002/joc.1173.

Brokmann, U., M. Jacquorie, M. Talkenberg, A. Harnisch, E.-W. Kreutz, D. Hülsenberg, and R. Poprawe (2002), Exposure of photosensitive glasses with pulsed UV-laser radiation, *Microsyst. Technol.*, *8*(2–3), 102–104, doi:10.1007/s00542-001-0134-x.

Brummer, G. J. A., C. Hemleben, and M. Spindler (1987), Ontogeny of extant spinose planktonic foraminifera (*Globigerinidae*): A concept exemplified by *Globigerinoides sacculifer* (Brady) and *G. ruber* (D'Orbigny), *Mar. Micropaleontol.*, *12*, 357–381.

Cember, R. P. (1988), On the sources, formation, and circulation of Red Sea deep water, *J. Geophys. Res.*, *93*, 8175–8191, doi:10.1029/JC093iC07p08175.

De Deckker, P. (2004), On the celestite-secreting Acantharia and their effect on seawater strontium to calcium ratios, *Hydrobiologia*, *517*(1–3), 1–13, doi:10.1023/B:HYDR.0000027333.02017.50.

De Nooijer, L. J., G. J. Reichart, A. Dueñas-Bohórquez, M. Wolthers, S. R. Ernst, P. R. D. Mason, and G. J. van der Zwaan (2007), Copper incorporation in foraminiferal calcite: Results from culturing experiments, *Biogeosci. Discuss.*, *4*(2), 961–991, doi:10.5194/bg-4-493-2007.

De Nooijer, L. J., E. C. Hathorne, G. J. Reichart, G. Langer, and J. Bijma (2014a), Variability in calcitic Mg/Ca and Sr/Ca ratios in clones of the benthic foraminifer *Ammonia tepida*, *Mar. Micropaleontol.*, *107*, 32–43, doi:10.1016/j.marmicro.2014.02.002.

De Nooijer, L. J., H. J. Spero, J. Erez, J. Bijma, and G. J. Reichart (2014b), Biomineralization in perforate foraminifera, *Earth Sci. Rev.*, *135*, 48–58, doi:10.1016/j.earscirev.2014.03.013.

De Villiers, S., M. Greaves and H. Elderfield (2002), An intensity ratio calibration method for the accurate determination of Mg/Ca and Sr/Ca of marine carbonates by ICP-AES, *Geochem. Geophys. Geosyst.*, *3*(1), 1001, doi:10.1029/2001GC000169.

Delaney, M. L., A. W. Bé, and E. A. Boyle (1985), Li, Sr, Mg, and Na in foraminiferal calcite shells from laboratory culture, sediment traps, and sediment cores, *Geochim. Cosmochim. Acta*, *49*(6), 1327–1341, doi:10.1016/0016-7037(85)90284-4.

Dissard, D., G. Nehrke, G. J. Reichart, and J. Bijma (2010), Impact of seawater pCO_2 on calcification and Mg/Ca and Sr/Ca ratios in benthic foraminiferal calcite: Results from culturing experiments with *Ammonia tepida*, *Biogeosciences*, *7*, 81–93, doi:10.1016/j.gca.2009.10.040.

Dueñas-Bohórquez, A., R. E. da Rocha, A. Kuroyanagi, J. Bijma, and G. J. Reichart (2009), Effect of salinity and seawater calcite saturation state on Mg and Sr incorporation in cultured planktonic foraminifera, *Mar. Micropaleontol.*, *73*(3), 178–189, doi:10.1016/j.marmicro.2009.09.002.

Dueñas-Bohórquez, A., R. E. Da Rocha, A. Kuroyanagi, L. J. De Nooijer, J. Bijma, and G. J. Reichart (2011), Interindividual variability and ontogenetic effects on Mg and Sr incorporation in the planktonic foraminifer *Globigerinoides sacculifer*, *Geochim. Cosmochim. Acta*, *75*(2), 520–532, doi:10.1016/j.gca.2010.10.006.

Eggins, S. M., A. Sadekov, and P. De Deckker (2004), Modulation and daily banding of Mg/Ca in *Orbulina universa* tests by symbiont photosynthesis and respiration: A complication for seawater thermometry?, *Earth Planet. Sci. Lett.*, *225*(3), 411–419, doi:10.1016/j.epsl.2004.06.019.

Elderfield, H., and G. Ganssen (2000), Past temperature and $\delta^{18}O$ of surface ocean waters inferred from foraminiferal Mg/Ca ratios, *Nature*, *405*(6785), 442–445, doi:10.1038/35013033.

Elderfield, H., M. Vautravers and M. Cooper (2002), The relationship between shell size and Mg/Ca, Sr/Ca, δ18O, and δ13C of species of planktonic foraminifera, *Geochem. Geophys. Geosyst.*, *3*(8), 1052, doi:10.1029/2001GC000194.

Evans, D., J. Erez, S. Oron, and W. Müller (2015), Mg/Ca-temperature and seawater-test chemistry relationships in the shallow-dwelling large benthic foraminifera *Operculina ammonoides*, *Geochim. Cosmochim. Acta*, *148*, 325–342, doi:10.1016/j.gca.2014.09.039.

Fallet, U., W. Boer, C. van Assen, M. Greaves, and G. J. A. Brummer (2009), A novel application of wet oxidation to retrieve carbonates from large organic-rich samples for ocean-climate research, *Geochem. Geophys. Geosyst.*, *10*, Q08004, doi:10.1029/2009GC002573.

Fallet, U., G. J. A. Brummer, J. Zinke, S. Vogels, and H. Ridderinkhof (2010), Contrasting seasonal fluxes of planktonic foraminifera and impacts on paleothermometry in the Mozambique Channel upstream of the Agulhas Current, *Paleoceanography*, *25*, PA4223, doi:10.1029/2010PA001942.

Fehrenbacher, J. S., H. J. Spero, A. D. Russell, L. Vetter, and S. Eggins (2015), Optimizing LA-ICP-MS analytical procedures for elemental depth profiling of foraminifera shells, *Chem. Geol.*, *407*, 2–9, doi:10.1016/j.chemgeo.2015.04.007.

Gat, J. R. (1996), Oxygen and hydrogen isotopes in the hydrologic cycle, *Ann. Rev. Earth Planet. Sci.*, *24*(1), 225–262, doi:10.1146/annurev.earth.24.1.225.

Golani, D. (1998), Impact of Red Sea fish migrants through the Suez Canal on the aquatic environment of the Eastern Mediterranean, *Bull. Ser. Yale School For. Environ. Stud.*, *103*, 375–387.

Gordon, C. M., R. A. Carr, and R. E. Larson (1970), The influence of environmental factors on the sodium and manganese content of barnacle shells, *Limnol. Oceanogr.*, *15*(3), 461–466, doi:10.4319/lo.1970.15.3.0461.

Hathorne, E. C., R. H. James, P. Savage, and O. Alard (2008), Physical and chemical characteristics of particles produced by laser ablation of biogenic calcium carbonate, *J. Anal. At. Spectrom.*, *23*(2), 240–243, doi:10.1039/B706727E.

Hathorne, E. C., et al. (2013), Interlaboratory study for coral Sr/Ca and other element/Ca ratio measurements, *Geochem. Geophys. Geosyst.*, *14*, 3730–3750, doi:10.1002/ggge.20230.

Hemleben, C., and J. Bijma (1994), Foraminiferal population dynamics and stable carbon isotopes, in *Carbon Cycling in the Glacial Ocean: Constraints on the Ocean's Role in Global Change*, pp. 145–166, Springer, Berlin Heidelberg, doi:10.1007/978-3-642-78737-9_7.

Hönisch, B., K. A. Allen, A. D. Russell, S. M. Eggins, J. Bijma, H. J. Spero, D. W. Lea, and J. Yu (2011), Planktic foraminifers as recorders of seawater Ba/Ca, *Mar. Micropaleontol.*, *79*(1), 52–57, doi:10.1016/j.marmicro.2011.01.003.

Hönisch, B., K. A. Allen, D. W. Lea, H. J. Spero, S. M. Eggins, J. Arbuszewski, P. de Menocal, Y. Rosenthal, A. D. Russell, and H. Elderfield (2013), The influence of salinity on Mg/Ca in planktic foraminifers—Evidence from cultures, core-top sediments and complementary $\delta^{18}O$, *Geochim. Cosmochim. Acta*, *121*, 196–213, doi:10.1016/j.gca.2013.07.028.

Hoogakker, B. A., G. P. Klinkhammer, H. Elderfield, E. J. Rohling, and C. Hayward (2009), Mg/Ca paleothermometry in high salinity environments, *Earth Planet. Sci. Lett.*, *284*(3), 583–589, doi:10.1016/j.epsl.2009.05.027.
Hülsenberg, D., A. Harnisch, and A. Bismarck (2008), *Microstructuring of Glasses*, pp. 11–15, Springer, Berlin Heidelberg.
Hurd, D. C. and D. W. Spencer (1991), *Marine Particles: Analysis and Characterization*, *Geophys. Monogr.*, vol. 63, AGU, Washington, D. C, doi:10.1029/GM063.
Ishikawa, M., and M. Ichikuni (1984), Uptake of sodium and potassium by calcite, *Chem. Geol.*, *42*(1), 137–146, doi:10.1016/0009-2541(84)90010-X.
Jochum, K. P., U. Weis, B. Stoll, D. Kuzmin, Q. Yang, I. Raczek, D. E. Jacob, A. Stracke, K. Birbaum, and D. Günther (2011), Determination of reference values for NIST SRM 610–617 glasses following ISO guidelines, *Geostand. Geoanal. Res.*, *35*(4), 397–429, doi:10.1111/j.1751-908X.2011.00120.x.
Kısakürek, B., A. Eisenhauer, F. Böhm, D. Garbe-Schönberg, and J. Erez (2008), Controls on shell Mg/Ca and Sr/Ca in cultured planktonic foraminiferan, *Globigerinoides ruber* (white), *Earth Planet. Sci. Lett.*, *273*, 260–269, doi:10.1016/j.epsl.2008.06.026.
Kitano, Y., M. Okumura, and M. Idogaki (1975), Incorporation of sodium, chloride and sulfate with calcium carbonate, *Geochem. J.*, *9*(2), 75–84.
Köhler-Rink, S., and M. Kühl (2005), The chemical microenvironment of the symbiotic planktonic foraminifer *Orbulina universa*, *Mar. Biol. Res.*, *1*(1), 68–78, doi:10.1080/17451000510019015.
Lea, D. W., and E. A. Boyle (1991), Barium in planktonic foraminifera, *Geochim. Cosmochim. Acta*, *55*(11), 3321–3331, doi:10.1016/0016-7037(91)90491-M.
Lea, D. W., T. A. Mashiotta, and Howard J. Spero (1999), Controls on magnesium and strontium uptake in planktonic foraminifera determined by live culturing, *Geochim. Cosmochim. Acta*, *63*(16), 2369–2379, doi:10.1016/S0016-7037(99)00197-0.
Lewis, E., and D. W. R. Wallace (1998), *Program Developed for CO_2 System Calculations, ORNL/CDIAC-105*, Carbon Dioxide Information Analysis Center, Oak Ridge Natl Lab., US Depart. of Energy, Oak Ridge, Tenn.
Li, Z., Z. Hu, Y. Liu, S. Gao, M. Li, K. Zong, H. Chen, and S. Hu (2015), Accurate determination of elements in silicate glass by nanosecond and femtosecond laser ablation ICP-MS at high spatial resolution, *Chem. Geol.*, *400*, 11–23, doi:10.1016/j.chemgeo.2015.02.004.
Morcos, S. A. (1970), Physical and chemical oceanography of the Red Sea, *Oceanogr. Mar. Biol. Ann. Rev.*, *8*, 73–202.
Munsel, D., U. Kramar, D. Dissard, G. Nehrke, Z. Berner, J. Bijma, G. J. Reichart, and T. Neumann (2010), Heavy metal incorporation in foraminiferal calcite: results from multi-element enrichment culture experiments with *Ammonia tepida*, *Biogeosciences*, *7*(8), 2339–2350, doi:10.5194/bg-7-2339-2010.
Nehrke, G., G. J. Reichart, P. Van Cappellen, C. Meile, and J. Bijma (2007), Dependence of calcite growth rate and Sr partitioning on solution stoichiometry: non-Kossel crystal growth, *Geochim. Cosmochim. Acta*, *71*(9), 2240–2249, doi:10.1016/j.gca.2007.02.002.
North, N. A. (1974), Pressure dependence of SrSO4 solubility, *Geochim. Cosmochim. Acta*, *38*(7), 1075–1081, doi:10.1016/0016-7037(74)90005-2.
Nürnberg, D., J. Bijma, and C. Hemleben (1996), Assessing the reliability of magnesium in foraminiferal calcite as a proxy for water mass temperatures, *Geochim. Cosmochim. Acta*, *60*(5), 803–814, doi:10.1016/0016-7037(95)00446-7.
Odum, H. T. (1951), Notes on the strontium contain of seawater, celestite Radiolaria and strontianite snail shell, *Science*, *114*, 211–213, doi:10.1126/science.114.2956.211.
Okai, T., A. Suzuki, H. Kawahata, S. Terashima, and N. Imai (2002), Preparation of a new geological survey of Japan geochemical reference material: Coral JCp-1, *Geostand. Newsl.*, *26*(1), 95–99, doi:10.1111/j.1751-908X.2002.tb00627.x.
Okumura, M., and Y. Kitano (1986), Coprecipitation of alkali metal ions with calcium carbonate, *Geochim. Cosmochim. Acta*, *50*(1), 49–58, doi:10.1016/0016-7037(86)90047-5.
Por, F. D. (2012), *Lessepsian Migration: The Influx of Red Sea Biota Into the Mediterranean by Way of the Suez Canal*, vol. 23, Springer Sci. & Business Media, Berlin Heidelberg.
Reichart, G. J., F. Jorissen, P. Anschutz, and P. R. Mason (2003), Single foraminiferal test chemistry records the marine environment, *Geology*, *31*(4), 355–358, doi:10.1130/0091-7613(2003)031<0355:SFTCRT>2.0.CO;2.
Rink, S., M. Kühl, J. Bijma, and H. J. Spero (1998), Microsensor studies of photosynthesis and respiration in the symbiotic foraminifer *Orbulina universa*, *Mar. Biol.*, *131*(4), 583–595, doi:10.1007/s002270050350.
Rohling, E. J. (1994), Glacial conditions in the Red Sea, *Paleoceanography*, *9*, 653–660, doi:10.1029/94PA01648.
Rohling, E. J. (2007), Progress in paleosalinity: Overview and presentation of a new approach, *Paleoceanography*, *22*, PA3215, doi:10.1029/2007PA001437.
Rohling, E. J., and G. R. Bigg (1998), Paleosalinity and $\delta^{18}0$: A critical assessment, *J. Geophys. Res.*, *103*, 1307–1318, doi:10.1029/97JC01047.
Rucker, J. B., and J. W. Valentine (1961), Salinity response of trace element concentration in *Crassostrea virginica*, *Nature*, *160*, 1099–1100, doi:10.1038/1901099a0.
Russell, A. D., B. Hönisch, H. J. Spero, and D. W. Lea (2004), Effects of seawater carbonate ion concentration and temperature on shell U, Mg, and Sr in cultured planktonic foraminifera, *Geochim. Cosmochim. Acta*, *68*(21), 4347–4361, doi:10.1016/j.gca.2004.03.013.
Sadekov, A., S. M. Eggins, P. De Deckker, and D. Kroon (2008), Uncertainties in seawater thermometry deriving from intratest and intertest Mg/Ca variability in *Globigerinoides ruber*, *Paleoceanography*, *23*, PA1215, doi:10.1029/2007PA001452.
Sarmiento, J. L., and N. Gruber (2006), *Ocean Biogeochemical Dynamics*, Princeton Univ. Press, Princeton, Woodstock.
Schouten, S., J. Ossebaar, K. Schreiber, M. V. M. Kienhuis, G. Langer, A. Benthien, and J. Bijma (2006), The effect of temperature, salinity and growth rate on the stable hydrogen isotopic composition of long chain alkenones produced by *Emiliania huxleyi* and *Gephyrocapsa oceanica*, *Biogeosciences*, *3*(1), 113–119, doi:10.5194/bg-3-113-2006.
Segev, E., and J. Erez (2006), Effect of Mg/Ca ratio in seawater on shell composition in shallow benthic foraminifera, *Geochem. Geophys. Geosyst.*, *7*, Q02P09, doi:10.1029/2005GC000969.
Siccha, M., G. Trommer, H. Schulz, C. Hemleben, and M. Kucera (2009), Factors controlling the distribution of planktonic foraminifera in the Red Sea and implications for the development of transfer functions, *Mar. Micropaleontol.*, *72*(3), 146–156, doi:10.1016/j.marmicro.2009.04.002.
Sofianos, S. S., W. E. Johns, and S. P. Murray (2002), Heat and freshwater budgets in the Red Sea from direct observations at Bab el Mandeb, *Deep Sea Res.*, *2*(49), 1323–1340, doi:10.1016/S0967-0645(01)00164-3.
Steinhardt, J., C. Cléroux, J. Ullgren, L. J. de Nooijer, J. V. Durgadoo, G. J. A. Brummer, and G. J. Reichart (2014), Anti-cyclonic eddy imprint on calcite geochemistry of several planktonic foraminiferal species in the Mozambique Channel, *Mar. Micropaleontol.*, *113*, 20–33, doi:10.1016/j.marmicro.2014.09.001.
Steinhardt, J., L. J. de Nooijer, G. J. Brummerand, and G. J. Reichart (2015), Profiling planktonic foraminiferal crust formation, *Geochem. Geophys. Geosyst.*, *16*, 2409–2430, doi:10.1002/2015GC005752.
Steinke, S., H. Y. Chiu, P. S. Yu, C. C. Shen, L. Löwemark, H. S. Mii, and M. T. Chen (2005), Mg/Ca ratios of two Globigerinoides ruber (white) morphotypes: Implications for reconstructing past tropical/subtropical surface water conditions, *Geochem. Geophys. Geosyst.*, *6*, Q11005, doi:10.1029/2005GC000926.

Thompson, P. R., A. W. Bé, J. C. Duplessy, and N. J. Shackleton (1979), Disappearance of pink-pigmented Globigerinoides ruber at 120,000 yr BP in the Indian and Pacific Oceans, *Nature*, *280*, 554–558, doi:10.1038/280554a0.

Wang, L. (2000), Isotopic signals in two morphotypes of Globigerinoides ruber (white) from the South China Sea: implications for monsoon climate change during the last glacial cycle, *Palaeogeogr. Palaeoclimatol. Palaeoecol.*, *161*(3), 381–394, doi:10.1016/S0031-0182(00)00094-8.

Wilson, S. A., A. E. Koenig, and R. Orklid (2008), Development of microanalytical reference material (MACS-3) for LA-ICP-MS analysis of carbonate samples, *Geochim. Cosmochim. Acta*, *72*, 1025.

Wit, J. C., L. J. de Nooijer, M. Wolthers, and G. J. Reichart (2013), A novel salinity proxy based on Na incorporation into foraminiferal calcite, *Biogeosciences*, *10*, 6375–6387, doi:10.5194/bg-10-6375-2013.

Yu, J., H. Elderfield, and B. Hönisch (2007), B/Ca in planktonic foraminifera as a proxy for surface seawater pH, *Paleoceanography*, *22*, PA2202, doi:10.1029/2006PA001347.

Zahn, R., and A. C. Mix (1991), Benthic foraminiferal $\delta^{18}O$ in the ocean's temperature-salinity-density field: Constraints on Ice Age thermohaline circulation, *Paleoceanography*, *6*, 1–20, doi:10.1029/90PA01882.

Zahran, M. A. (2010), *Climate-Vegetation: Afro-Asian Mediterranean and Red Sea Coastal Lands*, vol. 4, Springer Sci. & Business Media, Dordrecht, Netherlands, doi:10.1007/978-90-481-8595-5.